
A BAYESIAN APPROACH TO FUNCTIONAL REGRESSION: THEORY AND COMPUTATION

PREPRINT

✉ [José R. Berrendero](#)^{*1,2}, ✉ [Antonio Coín](#)^{†1}, and ✉ [Antonio Cuevas](#)^{‡1,2}

¹Departamento de Matemáticas, Universidad Autónoma de Madrid (UAM), Madrid, Spain

²Instituto de Ciencias Matemáticas ICMAT (CSIC-UAM-UC3M-UCM), Madrid, Spain

July 30, 2024

Abstract

We propose a novel Bayesian methodology for inference in functional linear and logistic regression models based on the theory of reproducing kernel Hilbert spaces (RKHS's). We introduce general models that build upon the RKHS generated by the covariance function of the underlying stochastic process, and whose formulation includes as particular cases all finite-dimensional models based on linear combinations of marginals of the process, which can collectively be seen as a dense subspace made of simple approximations. By imposing a suitable prior distribution on this dense functional space we can perform data-driven inference via standard Bayes methodology, estimating the posterior distribution through reversible jump Markov chain Monte Carlo methods. In this context, our contribution is two-fold. First, we derive a theoretical result that guarantees posterior consistency, based on an application of a classic theorem of Doob to our RKHS setting. Second, we show that several prediction strategies stemming from our Bayesian procedure are competitive against other usual alternatives in both simulations and real data sets, including a Bayesian-motivated variable selection method.

Keywords functional data analysis · functional regression · reproducing kernel Hilbert space · Bayesian inference · reversible jump MCMC · posterior consistency

1 Introduction

The problem of predicting a scalar response from a functional covariate is one that has gained traction over the last few decades, as more and more data is being generated with an ever-increasing level of granularity in the measurements. While in principle the functional data could simply be regarded as a discretized vector in a very high dimension, there are often many advantages in taking into account its functional nature, ranging from modeling the correlation among points that are close in the domain, to extracting information that may be hidden in the derivatives of the function in question. As a consequence, numerous proposals have arisen on how to suitably deal with functional data, all of them encompassed under the term Functional Data Analysis (FDA), which essentially explores statistical techniques to process, model and make inference on data varying over a continuum. A partial survey on such methods is Cuevas (2014) or Goia and Vieu (2016), while a more detailed exposition of the theory and applications can be found for example in Hsing and Eubank (2015).

FDA is undoubtedly an active area of research, which finds applications in a wide variety of fields, such as biomedicine, finance, meteorology or chemistry (Ullah and Finch, 2013). Accordingly, there are many recent contributions on how to tackle functional data problems, both from a theoretical and practical standpoint. Chief among them is the approach of reducing the problem to a finite-dimensional one, for example using a truncated

* joser.berrendero@uam.es

† antonio.coin@uam.es (corresponding author)

‡ antonio.cuevas@uam.es

basis expansion or spline interpolation methods (Müller and Stadtmüller, 2005; Aguilera and Aguilera-Morillo, 2013). At the same time, much effort has been put into building a sound theoretical basis for FDA, generalizing different frequentist concepts to the infinite-dimensional framework. Examples of this endeavor include the definition of centrality measures and depth-based notions for functional data (López-Pintado and Romo, 2009), functional ANOVA tests (Cuevas et al., 2004), a functional Mahalanobis distance (Galeano et al., 2015; Berrendero et al., 2020), or an extension of Fisher’s discriminant analysis for random functions (Shin, 2008), among many others. As the name suggests, FDA techniques are heavily inspired by functional analysis tools and methods: Hilbert spaces, linear operators, orthonormal bases, and so on. Incidentally, a notion that also intersects with the classical theory of machine learning and pattern recognition, and that has attained popularity in recent years, is that of reproducing kernel Hilbert spaces (RKHS’s) and their applications in functional data problems (e.g. Kupresanin et al., 2010; Yuan and Cai, 2010; Berrendero et al., 2018). On the other hand, Bayesian inference methods are ubiquitous in the realm of statistics, and though they also make use of random functions, the approach is slightly different from the FDA case. While there are recent works that offer a Bayesian treatment of functional data (e.g. Crainiceanu and Goldsmith, 2010; Shi and Choi, 2011), there is still no systematic approach to Bayesian methodologies within FDA. It is precisely at this relatively unexplored intersection between FDA and Bayesian methods that our work is aimed.

In particular, our goal is to study functional regression problems, the infinite-dimensional equivalents of the typical statistical regression problems, from a Bayesian perspective. We follow the path started by Ferguson (1974) of setting a prior distribution on a functional space and using the corresponding posterior for inference. In our case, we use a particular RKHS as the ambient space, resulting in functional regression models that allow for a simple yet efficient Bayesian treatment of functional data. Moreover, we also study the basic theoretical question of posterior consistency in these RKHS models within the proposed Bayesian framework. Consistency and posterior concentration are a type of frequentist validation criteria that have arguably been an active point of research in the last few decades, particularly in infinite-dimensional settings (Amewou-Atisso et al., 2003; Choi and Ramamoorthi, 2008), and also in the functional regression case (Lian et al., 2016; Abraham and Grollemund, 2020). To put it simply, posterior consistency ensures that with enough data points, the Bayesian updating mechanism works as intended and the posterior distribution eventually concentrates around the true value of the parameters, supposing the model is well specified. We leverage the properties of RKHS’s and existing techniques to show that posterior consistency holds in our models under some mild identifiability conditions, thus providing a coherent background to our Bayesian approach.

Finally, this theoretical side is complemented by extensive experimentation that showcases the application of the models in various prediction tasks. Following recent trends in Bayesian computation techniques, the posterior distribution is approximated via Markov chain Monte Carlo (MCMC) methods, specifically the *reversible jump* variant (RJMCMC) proposed by Green (1995). This computational work highlights the predictive performance of the proposed functional regression models, especially when compared with other usual frequentist methods.

L^2 -models, shortcomings and alternatives

In this work we are concerned with functional linear and logistic regression models, that is, situations where the goal is to predict a continuous or dichotomous variable from functional observations. Even though these problems can be formally stated with almost no differences from their finite-dimensional counterparts, there are some fundamental challenges as well as some subtle drawbacks that emerge as a result of working in infinite dimensions. To set a common framework, we will consider throughout a scalar response variable Y (either continuous or binary) which has some dependence on a stochastic L^2 -process $X = X(t) = X(t, \omega)$ with trajectories in $L^2[0, 1]$, observed on a dense grid. We will further suppose for simplicity that X is centered, that is, its mean function $m(t) = \mathbb{E}[X(t)]$ vanishes for all $t \in [0, 1]$. In addition, we will tacitly assume the existence of a labeled data set $\mathcal{D}_n = \{(X_i, Y_i) : i = 1, \dots, n\}$ of independent observations from (X, Y) , and our aim will be to accurately predict the response corresponding to unlabeled samples from X .

The most common scalar-on-function linear regression model is the classical L^2 -model, widely popularized since the first edition (1997) of the pioneering monograph by Ramsay and Silverman (2005). It can be seen as a generalization of the usual finite-dimensional model, replacing the scalar product in \mathbb{R}^d for that of the functional space $L^2[0, 1]$ (henceforth denoted by $\langle \cdot, \cdot \rangle$):

$$Y = \alpha_0 + \langle X, \beta \rangle + \varepsilon = \alpha_0 + \int_0^1 X(t)\beta(t) dt + \varepsilon, \quad (1.1)$$

where $\alpha_0 \in \mathbb{R}$, ε is a random error term independent from X with $\mathbb{E}[\varepsilon] = 0$, and the functional slope parameter $\beta = \beta(\cdot)$ is a member of the infinite-dimensional space $L^2[0, 1]$. In this case, the inference on β is hampered

by the fact that $L^2[0, 1]$ is an extremely broad space that contains many non-smooth or ill-behaved functions, so any estimation procedure involving optimization on it will typically be hard. In spite of this, model (1.1) is not flexible enough to include “simple” finite-dimensional models based on linear combinations of the marginals, such as $Y = \alpha_0 + \beta_1 X(t_1) + \dots + \beta_p X(t_p) + \varepsilon$ for some constants $\beta_j \in \mathbb{R}$ and instants $t_j \in [0, 1]$, which are especially appealing to practitioners confronted with functional data problems; see Berrendero et al. (2024) for additional details on this. Moreover, the non-invertibility of the covariance operator associated with X , which plays the role of the covariance matrix in the infinite case, invalidates the usual least squares theory (Cardot and Sarda, 2018). Thus, some regularization or dimensionality reduction technique is needed for parameter estimation; see Reiss et al. (2017) for a summary of several widespread methods.

A similar L^2 -based functional logistic equation can be derived for the binary classification problem via the logistic function:

$$\mathbb{P}(Y = 1 | X) = \frac{1}{1 + \exp\{-\alpha_0 - \langle X, \beta \rangle\}}, \quad (1.2)$$

where $\alpha_0 \in \mathbb{R}$ and $\beta \in L^2[0, 1]$. In this situation, the most common way of estimating the slope function β is via its maximum likelihood estimator (MLE). The same complications as in the linear case apply here, with the additional problem that in functional settings the MLE does not exist with probability one under fairly general conditions (see Berrendero et al., 2023).

It turns out that in both scenarios a natural alternative to the L^2 -model is the so-called reproducing kernel Hilbert space (RKHS) model, which instead assumes the unknown functional parameter β to be a member of the RKHS associated with the covariance function of the process X . As we will show later on, not only is this model simpler and arguably easier to interpret, but it also constrains the parameter space to smoother and more manageable functions. In fact, it does include a model based on finite linear combinations of the marginals of X as a particular case, while also generalizing the aforementioned L^2 -models under some conditions. These RKHS-based models and their idiosyncrasies have been explored in Berrendero et al. (2019, 2024) in the linear setting, and in Berrendero et al. (2023) in the logistic case.

A major aim of this work is to motivate these models inside the functional framework, while also providing efficient techniques to apply them in practice. Our main contribution is the proposal of a Bayesian approach for inference in these RKHS models, in which a prior distribution is imposed on β to use the posterior probabilities for prediction. Although setting a prior distribution on a functional space is generally a hard task, the specific parametric formulation we propose greatly facilitates this. Similar Bayesian schemes have recently been explored in Grollemund et al. (2019) and Abraham (2024), albeit not within a RKHS framework. Another set of techniques extensively studied in this context are variable selection methods, which aim to select the marginals $\{X(t_j)\}$ of the process that better summarize it according to some optimality criterion (see Ferraty et al., 2010 or Berrendero et al., 2016 by way of illustration). As it happens, some RKHS-based variable selection methods have already been proposed (e.g. Bueno-Larraz and Klepsch, 2019), but in general they have their own dedicated algorithms and procedures. As will shortly become apparent, our Bayesian methodology allows us to easily isolate the marginal posterior distribution corresponding to a finite set of points $\{t_j\}$, providing a Bayesian variable selection process along with the other prediction methods that naturally arise from the posterior.

Some essentials on RKHS's and notation

The methodology proposed in this work relies heavily on the use of RKHS's, so we outline the main characteristics of these spaces from a probabilistic point of view (for a more detailed account, see for example Berlinet and Thomas-Agnan, 2004). Let us denote by $K(t, s) = \mathbb{E}[X(t)X(s)]$ the covariance function of the centered process X , and in what follows suppose that it is continuous. To construct the corresponding RKHS $\mathcal{H}(K)$, we start by defining the functional space $\mathcal{H}_0(K)$ of all finite linear combinations of evaluations of K , that is,

$$\mathcal{H}_0(K) = \left\{ f \in L^2[0, 1] : f(\cdot) = \sum_{j=1}^p a_j K(t_j, \cdot), p \in \mathbb{N}, a_j \in \mathbb{R}, t_j \in [0, 1] \right\}. \quad (1.3)$$

This space is endowed with the inner product $\langle f, g \rangle_K = \sum_{i,j} a_i b_j K(t_i, s_j)$, given that $f(\cdot) = \sum_i a_i K(t_i, \cdot)$ and $g(\cdot) = \sum_j b_j K(s_j, \cdot)$. Then, $\mathcal{H}(K)$ is defined to be the completion of $\mathcal{H}_0(K)$ under the norm induced by the scalar product $\langle \cdot, \cdot \rangle_K$. As it turns out, functions in this space satisfy the so-called *reproducing property*: $\langle K(t, \cdot), f \rangle_K = f(t)$ for all $f \in \mathcal{H}(K)$ and $t \in [0, 1]$. An important consequence of this identity is that $\mathcal{H}(K)$ is a space of genuine functions and not of equivalence classes, since the values of the functions at specific points are in fact relevant, unlike in L^2 -spaces.

Now, a particularly useful approach in statistics is to regard $\mathcal{H}(K)$ as an isometric copy of a well-known space. Specifically, via *Loève's isometry* (Loève, 1948) one can establish a congruence Ψ_X between $\mathcal{H}(K)$ and the linear span of the process, $\mathcal{L}(X)$, in the space of all random variables with finite second moment, $L^2(\Omega)$ (see Lemma 1.1 in Lukić and Beder, 2001). This isometry is essentially the completion of the correspondence

$$\sum_{j=1}^p a_j X(t_j) \longleftrightarrow \sum_{j=1}^p a_j K(t_j, \cdot),$$

and can be formally defined, in terms of its inverse, as $\Psi_X^{-1}(U)(t) = \mathbb{E}[UX(t)]$ for $U \in \mathcal{L}(X)$. Despite the close connection between the process X and the space $\mathcal{H}(K)$, special care must be taken when dealing with concrete realizations, since in general the trajectories of X do not belong to the corresponding RKHS with probability one (Lukić and Beder, 2001, Corollary 7.1). As a consequence, the expression $\langle x, f \rangle_K$ is ill-defined and lacks meaning when x is a realization of X . However, following Parzen's approach in his seminal work (Parzen, 1961, Theorem 4E), we can leverage Loève's isometry and identify $\langle x, f \rangle_K$ with the image $\Psi_x(f) := \Psi_X(f)(\omega)$, for $x = X(\omega)$ and $f \in \mathcal{H}(K)$. This notation, viewed as a formal extension of the inner product, often proves to be useful and convenient.

Organization of the article

The rest of the paper is organized as follows. In Section 2 we explain the Bayesian methodology and the functional regression models we propose, including an overview of the reversible jump MCMC scheme. In Section 3 we derive a theoretical posterior consistency result. The empirical results of the experimentation are contained in Section 4, along with a short discussion of computational details. Lastly, the conclusions drawn from this work are presented in Section 5. Moreover, additional details and results are included in Appendices A, B, C and D.

2 A Bayesian methodology for RKHS-based functional regression models

The functional models contemplated here are those obtained by considering a functional parameter $\alpha \in \mathcal{H}(K)$ and replacing the scalar product for $\langle X, \alpha \rangle_K$ in the L^2 -models (1.1) and (1.2). As previously explained, this change in perspective has tangible benefits both in theory and practice on account of the RKHS properties. However, to further simplify things we will follow a parametric approach and suppose that α is in fact a member of the dense subspace $\mathcal{H}_0(K)$ defined in (1.3). Although natural in this context, this crucial assumption may seem too restrictive at first glance. Nonetheless, we will demonstrate that this scheme has a firm theoretical backing and that the resulting models perform sufficiently well in applied settings, seeming not to need the comprehensiveness (and complications) of the larger L^2 -spaces.

As we said before, with a slight abuse of notation we will understand the expression $\langle x, \alpha \rangle_K$ as $\Psi_x(\alpha)$, where $x = X(\omega)$ and Ψ_x is Loève's isometry. Hence, taking into account that $\alpha \in \mathcal{H}_0(K)$ and that $\Psi_X(K(t, \cdot)) = X(t)$ by definition, we can write $\langle x, \alpha \rangle_K \equiv \sum_j \beta_j x(t_j)$ when $\alpha(\cdot) = \sum_j \beta_j K(t_j, \cdot)$ and x is a realization of X . In this way we get a simpler, finite-dimensional approximation of the functional RKHS model, which we argue reduces the overall complexity while still capturing most of the relevant information. By restricting the ambient space to $\mathcal{H}_0(K)$ we are essentially truncating the value of p , the dimensionality, and thus advocating for parsimony. Moreover, the model remains "truly functional" in the sense that p is variable: we are exploiting the RKHS perspective to give a functional nature to *all* finite-dimensional models based on linear combinations of the marginals. Even though we are selecting a set of impact points $\{t_j\}$ that depends on the observed grid, we can circumvent problems with this approach by smoothing or interpolating the functional data in a pre-processing step.

In view of (1.3) and Loève's isometry, to set a prior distribution on the unknown function α (that is, a prior distribution on the functional space $\mathcal{H}_0(K)$) it suffices to consider a discrete distribution on the number of components p , and then impose p -dimensional continuous prior distributions on the coefficients β_j and the times t_j given p . Thanks to this parametric approach, the challenging task of setting a prior distribution on a space of functions is considerably simplified, while simultaneously not constraining the model to any specific distribution (in contrast to, say, Gaussian process regression methods). Moreover, note that our simplifying assumption on α is not actually very strong, since any prior distribution \mathbb{P}_0 on $\mathcal{H}_0(K)$ can be directly extended to a prior distribution \mathbb{P} on $\mathcal{H}(K)$: just define $\mathbb{P}(B) = \mathbb{P}_0(B \cap \mathcal{H}_0(K))$ for all Borel sets B on $\mathcal{H}(K)$.

Lastly, since the value of p can vary, we need a way to introduce dimension information in our MCMC posterior approximation scheme. There are several alternatives in the literature, such as product space

formulations (Carlin and Chib, 1995) or Bayesian averaging/model selection methods (Hoeting et al., 1999), but this is precisely the problem that reversible jump samplers were designed to solve. The use of these samplers fits naturally within our framework, as they allow the complexity of the model to be directly chosen by the data, jointly inferring about the dimensionality and the value of the parameters. We explore this approach in some detail in Section 2.3.

2.1 Functional linear regression

In the case of functional linear regression, the simplified RKHS model considered is

$$Y = \alpha_0 + \langle X, \alpha \rangle_K + \varepsilon = \alpha_0 + \sum_{j=1}^p \beta_j X(t_j) + \varepsilon, \quad (2.1)$$

where $\alpha(\cdot) = \sum_{j=1}^p \beta_j K(t_j, \cdot) \in \mathcal{H}_0(K)$, $\alpha_0 \in \mathbb{R}$, and $\varepsilon \sim \mathcal{N}(0, \sigma^2)$ is an error term independent from X . This model is essentially a finite-dimensional approximation from a functional perspective to the more general RKHS model that assumes $\alpha \in \mathcal{H}(K)$ (e.g. Berrendero et al., 2024). Since the number of components p is unknown, the full parameter space is $\Theta = \bigcup_{p \in \mathbb{N}} \Theta_p$, where $\Theta_p = \mathbb{R}^p \times [0, 1]^p \times \mathbb{R} \times \mathbb{R}^+$. In the sequel, a generic element of Θ_p will be denoted by $\theta_p = (\beta_1, \dots, \beta_p, t_1, \dots, t_p, \alpha_0, \sigma^2) \equiv (b_p, \tau_p, \alpha_0, \sigma^2)$, though we will occasionally omit the subscript when the value of p is understood. Before proceeding further, observe that we can rewrite model (2.1) in a more explicit and practical fashion in terms of the available sample information. For $\theta \in \Theta$, the reinterpreted model assumes the form

$$Y_i | X_i, \theta \stackrel{\text{ind.}}{\sim} \mathcal{N} \left(\alpha_0 + \sum_{j=1}^p \beta_j X_i(t_j), \sigma^2 \right), \quad i = 1, \dots, n. \quad (2.2)$$

It is worth mentioning that the model remains linear in the sense that it fundamentally involves a random variable $\langle X, \alpha \rangle_K = \Psi_X(\alpha)$ belonging to the linear span of the process X in $L^2(\Omega)$. Also, note that given the number of components p and the time instants t_j , the model becomes a multiple linear model with the $X(t_j)$ as scalar covariates. In fact, this RKHS model is particularly suited as a basis for variable selection methods (Berrendero et al., 2019), and furthermore the general RKHS model entails the classical L^2 -model (1.1) under certain conditions (see Berrendero et al., 2024). In addition, this model could be easily extended to the case of several covariates via an expression of type $Y = \alpha_0 + \Psi_{X^1}(\alpha_1) + \dots + \Psi_{X^q}(\alpha_q) + \varepsilon$. Then, as argued in Grollemund et al. (2019) for a similar situation, we could recover the full posterior by looking alternately at the posterior distribution of each covariate conditional on the rest of them.

Prior distributions

A simple and intuitive prior distribution for the parameter vector $\theta \in \Theta$, suggested by the structure of the parameter space and usually employed in the literature, is given by

$$\begin{aligned} p &\sim \pi(p), \\ t_j &\stackrel{\text{ind.}}{\sim} \mathcal{U}[0, 1], \quad j = 1, \dots, p, \\ \beta_j &\stackrel{\text{ind.}}{\sim} \mathcal{N}(0, \eta^2), \quad j = 1, \dots, p, \\ \pi(\alpha_0, \sigma^2) &\propto 1/\sigma^2, \end{aligned} \quad (2.3)$$

where $\pi(p)$ is any discrete distribution on \mathbb{N} (e.g. uniform on a given finite set) and $\eta^2 \in \mathbb{R}^+$ is a hyperparameter of the model that depends strongly on the expected scale of the data. On the one hand, note the use of a joint prior distribution on α_0 and σ^2 , which is a widely used non-informative prior known as Jeffrey's prior (Jeffreys, 1946). One should be wary of the Jeffreys-Lindley paradox when assigning improper priors (see Robert, 2014), but since all the parameters involved are common to all possible values of p , this formulation should not present difficulties. On the other hand, the prior on the coefficients β_j is deliberately kept simple and somewhat non-informative, as it will greatly speed up and simplify the computations of the RJMCMC sampler later on.

2.2 Functional logistic regression

In the case of functional logistic regression, we regard the binary response variable $Y \in \{0, 1\}$ as a Bernoulli random variable given the regressor $X = x \in L^2[0, 1]$, and as usual suppose that $\log(p(x)/(1-p(x)))$ is

linear in x , where $p(x) = \mathbb{P}(Y = 1 | X = x)$. Then, following the approach suggested by Berrendero et al. (2023), a simplified logistic RKHS model is given, in terms of the correspondence $\langle X, \alpha \rangle_K = \Psi_X(\alpha)$, by the equation

$$\mathbb{P}(Y = 1 | X) = \frac{1}{1 + \exp\{-\alpha_0 - \langle X, \alpha \rangle_K\}}, \quad \alpha_0 \in \mathbb{R}, \alpha \in \mathcal{H}_0(K). \quad (2.4)$$

Indeed, note that this can be seen as a finite-dimensional approximation (with a functional interpretation) to the general RKHS functional logistic model proposed by these authors, which can be obtained by replacing $\mathcal{H}_0(K)$ with $\mathcal{H}(K)$. Now, if we aim at a classification problem, our strategy will be similar to that followed in the functional linear model: after incorporating the sample information, we can rewrite (2.4) as

$$Y_i | X_i, \theta \stackrel{\text{ind.}}{\sim} \text{Bernoulli}(p_i), \quad i = 1, \dots, n, \quad (2.5)$$

with

$$p_i = \mathbb{P}(Y_i = 1 | X_i, \theta) = \frac{1}{1 + \exp\left\{-\alpha_0 - \sum_{j=1}^p \beta_j X_i(t_j)\right\}}, \quad i = 1, \dots, n,$$

where in turn $\alpha_0, \beta_j \in \mathbb{R}$ and $t_j \in [0, 1]$.

In much the same way as the linear regression model described above, this RKHS-based logistic regression model offers some advantages over the classical L^2 -model. First, it has a more straightforward interpretation and allows for a workable Bayesian approach. Secondly, it can be shown that under mild conditions the general RKHS logistic functional model holds whenever the conditional distributions $X|Y = i$ ($i = 0, 1$) are homoscedastic Gaussian processes, and in some cases it also entails the L^2 -model (see Berrendero et al., 2023); this arguably provides a solid theoretical motivation for the reduced model. Incidentally, these models also shed light on the near-perfect classification phenomenon for functional data, described by Delaigle and Hall (2012a) and further examined for example in the works of Berrendero et al. (2018) or Torrecilla et al. (2020).

Furthermore, a maximum likelihood approach for parameter estimation (although not considered here) is possible as well, since the finite-dimensional approximation mitigates the problem of non-existence of the MLE in the functional case. However, let us recall that even in finite-dimensional settings there are cases of quasi-complete separation in which the MLE does not exist (Albert and Anderson, 1984). Additionally, the non-existence issue of the MLE becomes more pronounced as the dimension increases, as exemplified in the theory recently developed by Candès and Sur (2020). In any event, we argue that the simplified RKHS model presented here is a compelling and feasible approach to functional logistic regression, since it bypasses the main difficulties of the usual maximum likelihood techniques.

Prior distributions

As far as prior distributions go, we proceed as we did in the linear model. However, following the advice in Gelman et al. (2008) and Ghosh et al. (2018) we do change the prior of the coefficients β_j and the constant α_0 , since their interpretation is different now:

$$\begin{aligned} p &\sim \pi(p), \\ t_j &\stackrel{\text{ind.}}{\sim} \mathcal{U}[0, 1], \quad j = 1, \dots, p, \\ \beta_j &\stackrel{\text{ind.}}{\sim} t_5(0, 2.5), \quad j = 1, \dots, p, \\ \alpha_0 &\sim \text{Cauchy}(0, 10). \end{aligned} \quad (2.6)$$

The scaled Student's t and Cauchy distributions represent a robust and weakly informative prior that provides shrinkage and can handle the case of separation in logistic regression. The specific values of the parameters have been chosen via experimentation following the initial recommendations in Ghosh et al. (2018), which also establishes the need to scale the regressors to have mean 0 and standard deviation 0.5. Lastly, note that in this case the nuisance parameter σ^2 does not appear.

2.3 Reversible jump samplers for prediction

For the inference step in our Bayesian procedure, the usual approach would be to consider a fixed number of components, chosen separately via some model selection criterion. Instead, we aim to construct a fully

Bayesian methodology that allows us to model the number of components and the component parameters jointly. Since we do not impose conjugate priors and the posterior distribution does not have a recognizable shape, a simple way to achieve the desired outcome is to use reversible jump MCMC (RJMCMC) techniques to approximate the posterior. Originally envisioned for approximate inference in Bayesian mixtures, they can be used to sample models with an unknown number of components, providing a certain level of flexibility and theoretically allowing the exploration of the whole parameter space (see Richardson and Green, 1997).

The basis of the RJMCMC mechanism is a clever reformulation of the standard MCMC technique: on each iteration, apart from updating the current parameters, it tries to increase or decrease the dimension, creating new components or eliminating some already present. The acceptance fraction for these new moves is selected so that detailed balance as a whole is maintained, but this includes the possibly challenging computation of a certain Jacobian that is the key to dimension matching (Green, 1995). However, in nested models such as ours, we can simplify this expression by only allowing on each iteration either the birth of a new component or the death of an existing one (i.e. changing the dimension by one unit at a time). If we also make the proposal distribution for the newly birthed components independent of previous values, the Jacobian term disappears, and the acceptance fraction reduces to (Brooks et al., 2003)

$$\alpha_{\text{nested}} = \min \left(1, \frac{\mathcal{L}(\theta_{p+1})}{\mathcal{L}(\theta_p)} \frac{\pi(\theta_{p+1})}{\pi(\theta_p)} \frac{b_{p,p+1}}{d_{p+1,p}} \frac{1}{q(\theta_{+1})} \right).$$

Here p is the current number of components, $b_{p,p+1}$ is the probability of increasing the dimension from p to $p+1$, $d_{p+1,p}$ is the probability of the reverse move (death), $q(\theta_{+1})$ is the proposal distribution for the added source, π is the prior probability and \mathcal{L} represents the likelihood. This is already a rather manageable expression that can be implemented efficiently, but we introduce another simplification: the proposal distribution is chosen to match the prior distribution, so that the corresponding terms cancel out. Nonetheless, in real-world scenarios one could consider more sophisticated proposal distributions that might better explore the parameter space; see for example Davies et al. (2023) or Korsakova et al. (2024) for some interesting ideas.

From a higher level perspective, the RJMCMC algorithm is an iterative procedure that produces a chain of M approximate samples $(p_m, \theta_{p_m}^*)$ of the posterior distribution $\pi(p, \theta_p | \mathcal{D}_n)$, each possibly of a different dimension; see Appendix C.3 for a visual representation. Given a previously unseen regressor X_{test} , with each of these samples we can generate an individual response following our RKHS models, denoted by $F(X_{\text{test}}, \theta_{p_m}^*)$. In the linear case we sample from $Y | X_{\text{test}}, \theta_{p_m}^*$ as in (2.2), and in the logistic case we directly consider the probabilities $\mathbb{P}(Y | X_{\text{test}}, \theta_{p_m}^*)$ in (2.5) instead. We propose to combine these predictions in four different ways.

One-stage methods

In these methods we essentially make use of the so-called posterior predictive distribution (PP), and they are in turn divided in two approaches.

(I) Weighted sum (W-PP). The first idea involves utilizing all available information by summarizing and aggregating every individual RKHS response. We start by considering a point summary statistic g (e.g. mean, median, mode) and consolidating the predictions from all sub-models, each having distinct dimension. Then, we bring together these predictions through a weighted sum, in which the weights correspond to the relative frequencies of the corresponding values of p :

$$\hat{Y} = \sum_p \tilde{\pi}(p | \mathcal{D}_n) g(\{F(X_{\text{test}}, \theta_{p_m}^*)\}_{m:p_m=p}),$$

where $\tilde{\pi}(p | \mathcal{D}_n) = M^{-1} \sum_m \mathbb{I}(p_m = p)$ and \mathbb{I} is the indicator function. Note that this approach is reminiscent of the factorization of the posterior distribution as $\pi(p, \theta_p | \mathcal{D}_n) = \sum_p \pi(p | \mathcal{D}_n) \pi(\theta_p | p, \mathcal{D}_n)$. Additionally, in the logistic case we employ the usual thresholding procedure to convert the final probability to a binary class label in $\{0, 1\}$. We shall see in Section 4 that this method produces the best results in practice.

(II) Maximum a posteriori (MAP-PP). We also consider a MAP strategy, where only the most probable sub-model is used and the rest of the samples are discarded. In this case, if $\bar{p} = \arg \max_p \tilde{\pi}(p | \mathcal{D}_n)$, predictions are computed as

$$\hat{Y} = g(\{F(X_{\text{test}}, \theta_{p_m}^*)\}_{m:p_m=\bar{p}}).$$

Although this method potentially ignores many samples in the posterior approximation, this omission may help reduce the noise and prevent outliers from affecting the final prediction.

Two-stage methods

In these methods we focus only on the marginal posterior distribution of $\tau_p = (t_1, \dots, t_p)$, disregarding the rest of the parameters and effectively constructing a variable selection procedure. After choosing a set of time instants $\{\hat{t}_j\}$ using the approximate posterior samples $\{\tau_{p_m}^*\}$, we can reduce the original regressors to just the marginals $\{X_i(\hat{t}_j)\}$ and apply any of the well-known finite-dimensional prediction algorithms suited for this situation. We have again two different strategies.

(III) Weighted sum (W-VS). We can mirror the weighted sum approach of the one-stage methods, with prediction computed as

$$\hat{Y} = \sum_p \tilde{\pi}(p | \mathcal{D}_n) H(X_{\text{test}}, \hat{\tau}_p),$$

where $\hat{\tau}_p = (\hat{t}_1, \dots, \hat{t}_p) = g(\{\tau_{p_m}^*\}_{m:p_m=p})$ and g is a component-wise summary statistic. The function H represents the prediction for X_{test} of a regular linear/logistic regression algorithm, fitted with the transformed data set $\{(X_i(\hat{\tau}_p), Y_i) : i = 1, \dots, n\}$. As before, in the logistic case the responses are thresholded to obtain a class label.

(IV) Maximum a posteriori (MAP-VS). We also consider a MAP approach to variable selection with only the information of the most probable model, i.e.,

$$\hat{Y} = H(X_{\text{test}}, \hat{\tau}_{\hat{p}}).$$

3 Posterior consistency

This section demonstrates how the RKHS-based Bayesian methodology proposed herein establishes a robust theoretical foundation for subsequent prediction procedures. Firstly, let us briefly recall what we understand by posterior consistency. Note that to avoid confusion, throughout this section we will sometimes use bold letters to represent random variables. Consider a sample space \mathcal{X} and X_1, \dots, X_n an i.i.d. sample of the data X . Let us fix a prior distribution Π for random variables θ on the parameter space Θ , that is, $\theta \sim \Pi$, and let P_θ represent a sampling model (a distribution on \mathcal{X} indexed by $\theta \in \Theta$) such that $X|\theta \sim P_\theta$. Furthermore, assume that the model is well-specified, i.e., there is a true value $\theta_0 \in \Theta$ such that $X \sim P_{\theta_0}$, and denote by P_0^∞ the joint probability measure of (X_1, X_2, \dots) when θ_0 is the true value of the parameter.

Definition 1 (Ghosh and Ramamoorthi, 2003). We say that the posterior distribution is (strongly) consistent at θ_0 if for every neighborhood U of θ_0 it holds that

$$\lim_{n \rightarrow \infty} \Pi(\theta \in U | X_1, \dots, X_n) = 1 \quad P_0^\infty - \text{a.s.}$$

For a metric space (Θ, d) , this is equivalent to

$$\lim_{n \rightarrow \infty} \Pi(d(\theta, \theta_0) < \varepsilon | X_1, \dots, X_n) = 1 \quad P_0^\infty - \text{a.s.}, \quad \text{for all } \varepsilon > 0.$$

Note that the conditional probabilities are computed under the assumed joint distribution of $(\theta, (X_1, X_2, \dots))$. Essentially, we are saying that the posterior concentrates around θ_0 for almost all sequences of data. Thus, if consistency holds, the effect of the prior gets diluted as more and more data is used for the inference.

Doob's theorem

It turns out that, under very general conditions, the posterior distribution is consistent at almost every value of θ_0 with respect to the measure induced by the prior (Doob, 1949). Let the sample space \mathcal{X} and the parameter space Θ be complete separable metric spaces, endowed with their respective Borel sigma-algebras. Consider the model $\theta \sim \Pi$ and $X_1, X_2, \dots | \theta \sim P_\theta$ i.i.d., where θ is a random variable taking values in Θ . Observe that this induces a posterior distribution $\Pi(\theta | X_1, \dots, X_n)$.

Theorem 2 (Doob's consistency theorem). *If $\theta \mapsto P_\theta$ is one-to-one and $\theta \mapsto P_\theta(A)$ is measurable for all measurable sets $A \subseteq \mathcal{X}$, then the posterior distribution is consistent at Π -almost all values of Θ . That is, there exists $\Theta_* \subseteq \Theta$ such that $\Pi(\Theta_*) = 1$ and for all $\theta_0 \in \Theta_*$, if $X_1, X_2, \dots \sim P_{\theta_0}$ i.i.d., then for any neighborhood B of θ_0 we have*

$$\lim_{n \rightarrow \infty} \Pi(\theta \in B | X_1, \dots, X_n) = 1 \quad P_0^\infty - \text{a.s.}$$

See chapter 1.3 of Ghosh and Ramamoorthi (2003) for more details on this result. As a side note, in a nonparametric setting where the object of interest is a random function (e.g. a probability density), there is also a stronger consistency result by Schwartz (1965) which omits the Π -almost sure qualification under some more restrictive conditions. Moreover, there are some extensions of this result that deal with independent but not identically distributed data (Choi and Ramamoorthi, 2008).

3.1 Consistency in our RKHS model

Now we study in detail how Doob's theorem can be applied in our linear RKHS model, but the posterior consistency results we obtain hold *mutatis mutandis* in the logistic case. In this section we will assume that the covariance function K of the underlying stochastic process X is strictly positive definite, which is not a very restrictive condition in practice. In the linear case the sample space is $\mathcal{X} \times \mathcal{Y} = L^2[0, 1] \times \mathbb{R}$, which is already a complete separable metric space. Next, consider for each $p \in \mathbb{N}$ the subset of the $(2p + 2)$ -Euclidean space $\Theta_p = \{(b, \tau, \alpha_0, \sigma^2) : b = (\beta_1, \dots, \beta_p) \in \mathbb{R}^p, \tau = (t_1, \dots, t_p) \in [0, 1]^p, \alpha_0 \in \mathbb{R}, \sigma^2 \in \mathbb{R}_0^+\}$. Then, we can write our infinite-dimensional parameter space as

$$\Theta = \bigcup_{p=1}^{\infty} \Theta_p. \quad (3.1)$$

At this point we can follow an approach very similar to the one in Miller (2023), where posterior consistency is established in a mixture model with an unknown number of components, which has an infinite-dimensional parameter space that factorizes in the same way as (3.1). Note that given $\theta \in \Theta$ there is a unique $p = p(\theta)$ such that $\theta \in \Theta_p$. Considering that we will only be interested in small balls around the true value of the parameter, we can define a metric for $\theta, \theta' \in \Theta$ by

$$d(\theta, \theta') = \begin{cases} \min\{\|\theta - \theta'\|, 1\}, & \text{if } p(\theta) = p(\theta'), \\ 1, & \text{otherwise.} \end{cases} \quad (3.2)$$

Since each Θ_p is itself a complete separable metric space with the inherited Euclidean norm, Proposition A.1 in Miller (2023) ensures that (Θ, d) is a complete separable metric space. Further, we equip both $\mathcal{X} \times \mathcal{Y}$ and Θ with their respective Borel sigma-algebras.

In terms of $\theta \in \Theta$, the data distribution is $P_\theta(X, Y) = P_{b, \tau, \alpha_0, \sigma^2}(X, Y)$, and formally the joint distribution $P_\theta(X, Y)$ factorizes as $P_\theta(X, Y) = P(X)P_\theta(Y|X)$. Here $P(X)$ is the distribution of the underlying process X , and in our RKHS setting, $P_\theta(Y|X) \equiv \mathcal{N}(\alpha_0 + \sum_{j=1}^{p(\theta)} \beta_j X(t_j), \sigma^2)$. Now, let us suppose that $\theta \mapsto P_\theta(X, Y)(A)$ is measurable for all measurable sets $A \subseteq \mathcal{X} \times \mathcal{Y}$, which is true under mild conditions (see Appendix B). Moreover, for convenience, we will denote the sequences $(X, Y)_{1:n} = (X_1, Y_1), \dots, (X_n, Y_n)$ and $(X, Y)_{1:\infty} = (X_1, Y_1), (X_2, Y_2), \dots$

Now, the full hierarchical model under consideration is

$$\begin{aligned} (\text{no. of components}) \quad & \mathcal{P} \sim \pi, \\ (\text{component values}) \quad & \mathbf{b} \mid \mathcal{P} = p \sim F_p, \\ (\text{component times}) \quad & \boldsymbol{\tau} \mid \mathcal{P} = p \sim G_p, \\ (\text{intercept}) \quad & \alpha_0 \sim C, \\ (\text{error variance}) \quad & \sigma^2 \sim D, \\ (\text{observed data}) \quad & (X, Y)_{1:n} \mid \mathbf{b}, \boldsymbol{\tau}, \alpha_0, \sigma^2 \sim P_{\mathbf{b}, \boldsymbol{\tau}, \alpha_0, \sigma^2}(X, Y) \quad \text{i.i.d.}, \end{aligned} \quad (3.3)$$

where π, F_p, G_p, C and D are probability measures on $\mathbb{N}, \mathbb{R}^p, [0, 1]^p, \mathbb{R}$ and \mathbb{R}_0^+ , respectively. Note that since $P_\theta(X, Y)$ is invariant under permutations of the component labels b and τ , we can only show consistency up to one such permutation. To that effect, and mirroring the strategy in Miller (2023), let S_p denote the set of permutations of $\{1, \dots, p\}$, and for $\nu \in S_p$ and $\theta \in \Theta_p$, denote by $\theta[\nu]$ the result of applying the permutation ν to the component labels of θ . That is, if $\theta = (\beta_1, \dots, \beta_p, t_1, \dots, t_p, \alpha_0, \sigma^2)$, then $\theta[\nu] = (\beta_{\nu_1}, \dots, \beta_{\nu_p}, t_{\nu_1}, \dots, t_{\nu_p}, \alpha_0, \sigma^2)$. Next, define $\tilde{B}(\theta_0, \varepsilon) = \bigcup_{\nu \in S_p} \{\theta \in \Theta : d(\theta, \theta_0[\nu]) < \varepsilon\}$ for $\theta_0 \in \Theta_p$ and $\varepsilon > 0$, which is the set of all parameters that are within ε of some permutation of (the component labels of) θ_0 . Lastly, define the random variable $\boldsymbol{\theta} = (\mathbf{b}, \boldsymbol{\tau}, \alpha_0, \sigma^2)$, which takes values in Θ , and denote by Π the prior distribution on $\boldsymbol{\theta}$ implied by the model in (3.3). In order for identifiability to hold, we need to place some restrictions on the prior:

Condition 3 (Identifiability constraints). Under the model in (3.3), for all $p \in \mathbb{N}$:

- (i) $\Pi(t_i = t_j | \mathcal{P} = p) = 0$ for all $1 \leq i < j \leq p$.
- (ii) There exists $\delta > 0$ such that $\Pi(|\beta_j| < \delta | \mathcal{P} = p) = 0$ for all $1 \leq j \leq p$.

Both assumptions can be interpreted as a way of pursuing parsimony in the model, aiming for as few components as possible. In practical and computational terms, we can think of δ as the *machine precision number*, so that virtually all continuous prior distributions satisfy the associated condition when implemented numerically in a computer. With this setup in mind, we are now ready to state our main consistency result:

Theorem 4. *Suppose that Condition 3 holds. Then there exists $\Theta_* \subseteq \Theta$ such that $\Pi(\theta \in \Theta_*) = 1$ and for all $\theta_0 \in \Theta_*$, if $(X, Y)_{1:\infty} \sim P_{\theta_0}(X, Y)$ i.i.d., then for all $\varepsilon > 0$*

$$\lim_{n \rightarrow \infty} \Pi(\theta \in \tilde{B}(\theta_0, \varepsilon) \mid (X, Y)_{1:n}) = 1 \quad P_0^\infty(X, Y) - a.s.$$

and

$$\lim_{n \rightarrow \infty} \Pi(\mathcal{P} = p(\theta_0) \mid (X, Y)_{1:n}) = 1 \quad P_0^\infty(X, Y) - a.s.$$

The second conclusion is of certain relevance in itself, because the estimation of the number of components in mixture-like models is a hard problem in general (see Miller and Harrison, 2018, and references therein). Moreover, it is worth pointing out that the proof of Theorem 4 can be easily adjusted to guarantee consistency when the number of components is fixed beforehand (and thus the parameter space is finite-dimensional). Indeed, in this case Doob's theorem applies directly under the sole condition that the times be distinct with prior probability one. The coefficients β_j do not cause a problem for identifiability now, since the dimension of every parameter is the same.

Corollary 5. *Assume model (3.3) in which the value of p is fixed, and hence Θ_p is the (finite-dimensional) parameter space. Suppose that Condition 3-(i) holds as well. Then, if θ_0 is the true value of the parameter, the posterior is consistent at θ_0 with Π -probability one.*

Note that by allowing β_j to be zero in this situation we can sometimes circumvent the fact that the true value of the parameter might not have exactly p components, as long as p is larger than the true value $p(\theta_0)$. Indeed, if $\theta_0 \in \Theta$ with $p(\theta_0) < p$ and $(X, Y)_{1:\infty} \sim P_{\theta_0}(X, Y)$ i.i.d., then we can find $\theta_1 \in \Theta_p$, which is just θ_0 completed with zeros, such that $P_{\theta_0}(X, Y) = P_{\theta_1}(X, Y)$ and the result holds almost surely.

A remark on Lebesgue consistency

All in all, Theorem 4 guarantees consistency for Π -almost every parameter in the support of the prior distribution. However, even though we can choose the prior so that $\text{supp}(\Pi) = \Theta$, in principle there is no assurance that the Π -null set in which consistency may fail will not be a large set with respect to other (e.g. Lebesgue) measures. In fact, when the parameter space is infinite-dimensional there are examples of big inconsistency sets, even for reasonably chosen prior distributions (Diaconis and Freedman, 1986). Nonetheless, this problem can be alleviated when the parameter space is a countable union of disjoint finite-dimensional sets, as we can further refine our almost sure statement. First, note that there is a natural extension of the Lebesgue measure to our parameter space Θ : just consider the genuine Lebesgue measure λ_p on Θ_p , and for all $B \subseteq \Theta$ measurable define $\lambda(B) = \sum_{p=1}^{\infty} \lambda_p(\Theta_p \cap B)$. Then, if we choose a prior distribution with respect to which this measure is absolutely continuous, the consistency set Θ_* in Theorem 4 will satisfy $\lambda(\Theta \setminus \Theta_*) = 0$. A similar approach is considered in Nobile (1994) and Miller (2023) to establish ‘‘Lebesgue’’-almost sure consistency in finite mixture models with a prior on the number of components. In our case, the requirement of absolute continuity can be relaxed so that sets with nonzero Lebesgue measure have nonzero prior probability for some permutation of the component labels. We give more details on this result in Appendix B.

3.2 A sketch of the proof

We now present a proof of our consistency result. The general strategy will be to apply Doob's theorem to a subset of the parameter space Θ , where permutations are suitably taken into account and full identifiability holds, and then extend the conclusions to the whole parameter space. As we will see shortly, save for an eventual permutation, identifiability of the map $\theta \mapsto P_\theta(X, Y)$ is obtained in the RKHS case when the covariance function K of the underlying stochastic process is non-degenerate.

Reduced parameter space. Consider the space $\mathbb{R}_\delta = (-\infty, -\delta] \cup [\delta, +\infty)$, with δ the fixed tolerance given in Condition 3-(ii), and define

$$\tilde{\Theta}_p = \mathbb{R}_\delta^p \times [0, 1]_{\text{ord}}^p \times \mathbb{R} \times \mathbb{R}_0^+,$$

where $[0, 1]_{\text{ord}}^p = \{(t_1, \dots, t_p) \in [0, 1]^p : t_1 < \dots < t_p\}$. Now consider $\tilde{\Theta} = \bigcup_{p \in \mathbb{N}} \tilde{\Theta}_p$, and note that the sets $\tilde{\Theta}_1, \tilde{\Theta}_2, \dots$ are still disjoint. Then, again by Proposition A.1 in Miller (2023), we can conclude that $\tilde{\Theta}$ is a complete separable metric space under the metric d in (3.2). We will henceforth say that a parameter in $\tilde{\Theta}$ is “ordered”.

Transformation into ordered form. For $\theta \in \Theta_p$, define $T(\theta) = \theta[\nu]$ if there is a $\nu \in S_p$ such that $\theta[\nu] \in \tilde{\Theta}_p$; otherwise set $T(\theta) = \theta$. Note that we can only transform θ to be in $\tilde{\Theta}_p$ if the times t_j are all distinct and the coefficients β_j satisfy $|\beta_j| \geq \delta$. But since the prior distribution assigns probability one to both events by Condition 3, we have $\Pi(T(\theta) \in \tilde{\Theta}) = 1$. It will be useful later to observe that for any set $B \subseteq \tilde{\Theta}_p$, if we denote $B[\nu] = \{\theta[\nu] : \theta \in B\}$, we have

$$\bigcup_{\nu \in S_p} B[\nu] = T^{-1}(B). \quad (3.4)$$

Collapsed model. Note that $P_{T(\theta)}(X, Y) = P_\theta(X, Y)$, and let \tilde{Q} denote the distribution of $T(\theta)$ restricted to $\tilde{\Theta}$. Then the following model holds on the reduced space $\tilde{\Theta}$:

$$\begin{aligned} T(\theta) &\sim \tilde{Q}, \\ (X, Y)_{1:n} \mid T(\theta) &\sim P_{T(\theta)}(X, Y) \quad \text{i.i.d.} \end{aligned} \quad (3.5)$$

Verifying conditions. We will now show that the conditions of Doob’s theorem hold on $\tilde{\Theta}$. First, since $\theta \mapsto P_\theta(X, Y)(A)$ is measurable on Θ , it is also measurable on $\tilde{\Theta}$ for all sets $A \subseteq \mathcal{X} \times \mathcal{Y}$ measurable. For the identifiability part, suppose by contradiction that there are two parameters $\theta, \theta' \in \tilde{\Theta}$ such that $\theta \neq \theta'$ and $P_\theta(X, Y) = P_{\theta'}(X, Y)$. Then necessarily $P_\theta(Y|X) = P_{\theta'}(Y|X)$, which in turn implies that the means and variances of these distributions are equal, i.e., $\sigma^2 = (\sigma')^2$ and

$$\alpha_0 + \sum_{j=1}^{p(\theta)} \beta_j X(t_j) = \alpha'_0 + \sum_{j=1}^{p(\theta')} \beta'_j X(t'_j),$$

where $t_i \neq t_j$ and $t'_i \neq t'_j$ for $i \neq j$. Reordering the terms and combining those where the impact points coincide, this means that a linear combination of marginals of the process X equals a constant. By taking variances, we can see that all the coefficients in this linear combination must vanish, since the covariance function of the process is strictly positive definite. But β_j and β'_j cannot be 0 for any j (by definition of $\tilde{\Theta}$), so it must be the case that $\theta' = \theta[\nu]$ for some $\nu \in S_p$, where $p = p(\theta) = p(\theta')$. However, $t_1 < \dots < t_p$ and $t'_1 < \dots < t'_p$, so ν must be the identity permutation, that is, $\theta' = \theta$, contradicting the initial assumption.

Applying Doob’s theorem. Next we analyze the conclusions of Doob’s theorem applied to the collapsed model (3.5): there exists $\tilde{\Theta}_* \subseteq \tilde{\Theta}$ with $\Pi(T(\theta) \in \tilde{\Theta}_*) = 1$ such that, if $T(\theta_0) \in \tilde{\Theta}_*$ and it holds that $(X, Y)_{1:\infty} \sim P_{T(\theta_0)}(X, Y)$ i.i.d., then for any neighborhood $B \subseteq \tilde{\Theta}$ of $T(\theta_0)$ we have

$$\Pi(T(\theta) \in B \mid (X, Y)_{1:n}) \xrightarrow{n \rightarrow \infty} 1 \quad P_{T(\theta_0)}^\infty - \text{a.s.} \quad (3.6)$$

Now define Θ_* to be the set of all parameters in Θ that can be obtained by permuting a parameter in $\tilde{\Theta}_*$, i.e., $\Theta_* = \bigcup_{p=1}^\infty \bigcup_{\nu \in S_p} (\tilde{\Theta}_* \cap \tilde{\Theta}_p)[\nu]$. Then, by (3.4) we get

$$\Pi(\theta \in \Theta_*) = \Pi\left(T(\theta) \in \bigcup_{p=1}^\infty (\tilde{\Theta}_* \cap \tilde{\Theta}_p)\right) = \Pi(T(\theta) \in \tilde{\Theta}_*) = 1.$$

Extending the result to Θ . Let $\theta_0 \in \Theta_*$, suppose that $(X, Y)_{1:\infty} \sim P_{\theta_0}(X, Y)$ i.i.d., and define $p_0 = p(\theta_0)$ and $S_0 = S_{p_0}$. Fix $\varepsilon \in (0, 1)$ and consider the set B of all ordered parameters that are within ε of the ordered version of θ_0 , i.e.,

$$B = \left\{ \theta \in \tilde{\Theta} : d(\theta, T(\theta_0)) < \varepsilon \right\}. \quad (3.7)$$

Observe that, since $\varepsilon < 1$, we have $B \subseteq \tilde{\Theta}_{p_0}$ by definition of d . Moreover, $\bigcup_{\nu \in S_0} B[\nu] \subseteq \tilde{B}(\theta_0, \varepsilon)$. Then, again by (3.4), we can write

$$\begin{aligned} \Pi(\theta \in \tilde{B}(\theta_0, \varepsilon) \mid (X, Y)_{1:n}) &\geq \Pi(\theta \in \bigcup_{\nu \in S_0} B[\nu] \mid (X, Y)_{1:n}) \\ &= \Pi(T(\theta) \in B \mid (X, Y)_{1:n}). \end{aligned} \quad (3.8)$$

Now, $T(\theta_0) \in \tilde{\Theta}_*$ because $\theta_0 \in \Theta_*$, and in that case we know that the collapsed model is consistent at $T(\theta_0)$. Note that we also have $(X, Y)_{1:\infty} \sim P_{T(\theta_0)}(X, Y)$ i.i.d. (since $P_{\theta_0} = P_{T(\theta_0)}$), and the set B in (3.7) is a neighborhood of $T(\theta_0)$ in $\tilde{\Theta}$. Then, by (3.6), we have $\Pi(T(\theta) \in B \mid (X, Y)_{1:n}) \xrightarrow{n \rightarrow \infty} 1$, $P_{\theta_0}^\infty(X, Y) - \text{a.s.}$, and this fact together with (3.8) proves consistency for θ_0 in the original model (3.3). Lastly, since $\varepsilon < 1$ implies $\tilde{B}(\theta_0, \varepsilon) \subseteq \Theta_{p_0}$, we have also proved the second assertion of our theorem:

$$\begin{aligned} \Pi(\mathcal{P} = p_0 \mid (X, Y)_{1:n}) &= \Pi(\theta \in \Theta_{p_0} \mid (X, Y)_{1:n}) \\ &\geq \Pi(\theta \in \tilde{B}(\theta_0, \varepsilon) \mid (X, Y)_{1:n}) \\ &\xrightarrow{n \rightarrow \infty} 1 \quad P_{\theta_0}^\infty(X, Y) - \text{a.s.} \quad \square \end{aligned}$$

As a final comment, it is worth reiterating that in this theoretical aspect of our work we have closely followed the techniques recently developed in Miller (2023), where the author provides a simplification of the work by Nobile (1994) in studying posterior consistency in finite-dimensional mixture models with a prior on the number of components. While the methods are quite similar, we have succeeded in extending this theory to a fundamentally different situation, namely functional regression, which thanks to the RKHS formulation shares the key properties that allow for a treatment analogous to the finite-dimensional mixture case.

4 Experimental results

In this section we present the results of the experiments carried out to test the performance of our Bayesian methods in different scenarios, together with an overview of their computational implementation. Further details such as simulation parameters or algorithmic decisions, as well as additional experiments, figures and tables are provided in Appendices A, C and D, while the code itself is publicly available on GitHub at <https://github.com/antcc/rk-bfr-jump>.

For simulated data we consider $n = 200$ training samples and $n' = 100$ testing samples on an equispaced grid of 100 points on $[0, 1]$, and for the real data sets we perform a 66%/33% train/test split. We fit our models on the training data, using RJMCMC to approximate the posterior, and then use the test set for out-of-sample predictions. We independently repeat the whole process 10 times (each with a different train/test configuration) to account for the stochasticity in the sampling step, and average the results across these executions. For the purposes of prediction we consider the point statistics *trimmed mean* (10%), *median* and *mode* to aggregate together predictions and summarize parameters (see Section 2.3). Moreover, the values of $\{t_j\}$ that fall outside the specified grid are truncated to the nearest neighbor in the grid, with the additional restriction that time instants in different components of our models cannot be equal.

The Python library used to perform the RJMCMC approximation is *Eryn* (Karnesis et al., 2023). It is a toolbox for Bayesian inference that allows trans-dimensional posterior approximation, running multiple chains in an ensemble configuration with different starting points, and incorporating a parallel tempering mechanism (Hukushima and Nemoto, 1996) to increase both convergence speed and the acceptance rate. Because of execution time constraints, the hyperparameters of the Eryn sampler are selected manually based on an initial set of experiments, as well as recommendations from the authors. Moreover, some amount of post-processing is needed to mitigate the well-known *label switching* phenomenon that occurs in MCMC approximations of mixture-like models (Stephens, 2000); see Appendix A.2.

Data sets

We consider a set of functional regressors common to linear and logistic regression problems. They are four zero-mean Gaussian processes (GPs), each with a different covariance function. In particular, we consider a Brownian motion, a fractional Brownian motion, an Ornstein-Uhlenbeck process, and a GP with a squared exponential kernel.

Linear regression data sets. We employ two different types of simulated data sets, all with a common value of $\alpha_0 = 5$ and $\sigma^2 = 0.5$:

- A finite-dimensional RKHS response with three components for each of the four GP regressors mentioned above: $Y = 5 - 5X(0.1) + 5X(0.6) + 10X(0.8) + \varepsilon$.
- A “component-less” response generated by an L^2 -model with a smooth underlying coefficient function, namely $\beta(t) = \log(1 + 4t)$, again for the same four GPs.

As for the real data sets, we use the Tecator data set (Borggaard and Thodberg, 1992) to predict fat content based on near-infrared absorbance curves of 193 meat samples, as well as what we call the Moisture (Kalivas, 1997) and Sugar (Bro, 1999) data sets. The first consists of near-infrared spectra of 100 wheat samples and the objective is to predict the samples’ moisture content, whereas the second contains 268 samples of sugar fluorescence data in order to predict ash content. The regressors of the three data sets are measured on a grid of 100, 101 and 115 equispaced points on $[0, 1]$, respectively.

Logistic regression data sets. Again we consider two different types of simulated data sets, with a common value of $\alpha_0 = -0.5$:

- Four logistic finite-dimensional RKHS responses with the same functional parameter as in the linear regression case (one for each GP). Specifically,

$$\mathbb{P}(Y = 1 \mid X) = \frac{1}{1 + \exp\{0.5 + 5X(0.1) - 5X(0.6) - 10X(0.8)\}}.$$

- Four logistic responses following an L^2 -model with the same coefficient function as in the linear regression case, i.e., $\beta(t) = \log(1 + 4t)$.

Additionally, we use three real data sets well known in the literature. The first one is a subset of the Medflies data set (Carey et al., 1998), consisting on samples of the number of eggs laid daily by 534 flies over 30 days, to predict whether their longevity is high or low. The second one is the Berkeley Growth Study data set (Tuddenham and Snyder, 1954), which records the height of 54 girls and 39 boys over 31 different points in their lives. Finally, we selected a subset of the Phoneme data set (Hastie et al., 1995), based on 200 digitized speech frames over 128 equispaced points to predict the phonemes “aa” and “ao”.

Comparison algorithms

We have included a fairly comprehensive suite of comparison algorithms, chosen among the most common frequentist methods used in machine learning and FDA, and following a standard choice of implementation and hyperparameters. There are purely functional methods (such as the usual L^2 regression based on model (1.1)), finite-dimensional models that work on the discretized data (e.g. penalized finite-dimensional regression), and variable selection/dimension reduction procedures (like Principal Component Analysis or Partial Least Squares). The main parameters of all these algorithms are selected by cross-validation, and when a number of components needs to be specified, we use the same range as in our own models so that comparisons are fair. A more detailed account of these algorithms is available in Appendix C.1.

Results display

We have adopted a visual approach to presenting the experimentation results, using colored graphs to help visualize them. In each case, the mean and standard deviation of the score obtained across the 10 random runs is shown, depicting our methods in blue and the comparison algorithms in orange. We also show the global mean of all the comparison algorithms with a dashed vertical line, excluding extreme negative results to avoid distortion. Moreover, we separate one-stage and two-stage methods, the latter being the ones that perform variable selection or dimension reduction prior to a multiple linear/logistic regression method (represented with “+r”/“+log” in the figures). We name our methods according to the acronyms described in Section 2.3.

4.1 Functional linear regression

The initial experiments carried out indicate that low values of p provide sufficient flexibility in most scenarios, so we allow the number of components to vary in the set $\{1, 2, \dots, 10\}$. Following Nobile and Fearnside (2007) we select a truncated Poisson prior with a low rate parameter $\lambda = 3$ for p , so that simpler models are

avored. However, in the experiments with real data we set $p \sim \mathcal{U}\{1, 2, \dots, 10\}$ to allow a less informative exploration of the parameter space. Moreover, for simplicity we choose to scale the regressors and response to have standard deviation unity in the inference step, but then convert the results back to the original scale for prediction. This allows us to set a reasonable value of $\eta^2 = 25$ in the weakly informative prior of β_j (see (2.3)). Lastly, the metric used to evaluate the performance is the Root Mean Square Error (RMSE).

Simulated data sets

In Figure 1 we see the results for the RKHS response. This is our baseline and the most favorable case for us, as the underlying model coincides with our assumed model. Indeed, we can see that in most instances our algorithms are the ones with lower RMSE, as expected, and there is not much variance among our different approaches to prediction, at least in the one-stage methods. We even manage to consistently beat the *lasso* finite-dimensional regression mechanism, which can select all 100 components for its model, versus our 10 components at most. This is an indicator that our models make a more efficient selection of variables, encapsulating more information with fewer components and justifying our partiality to parsimonious models.

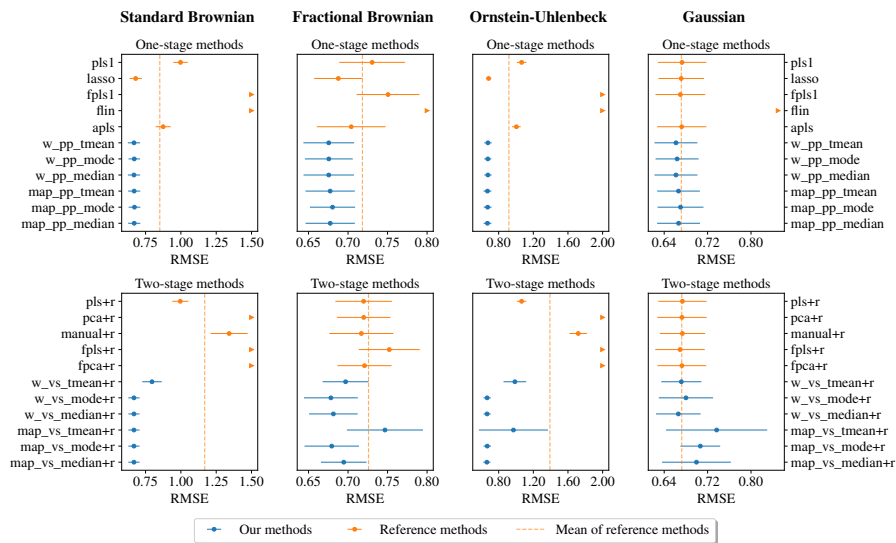


Figure 1: Mean and standard error of RMSE of predictors (lower is better) for 10 runs with GP regressors, one on each column, that obey an underlying linear RKHS model.

Figure 2 shows the results for an underlying L^2 -model, which would be our direct competitor and a more representative test for our Bayesian model. In this case the outcome is satisfactory, as for the most part our models are on a par with the rest, even defeating other methods that were designed with the L^2 -model in mind. Especially interesting is the comparison with the standard L^2 functional regression (*flin* in the graphics), which we outperform most of the time.

Real data

Figure 3 depicts the results for the real data sets, where we can see that the performance of our one-stage methods is about the same as that of the comparison methods. However, our variable selection methods are somewhat worse than the reference methods, although not by a wide margin. We have to bear in mind that real data is more complex and noisy than simulated data, and it is possible that after a suitable pre-preprocessing we would have obtained better results. Nonetheless, our goal was to perform a general comparison with a uniform methodology, without focusing too much on the specifics of any particular data set.

On another note, we see that some of our Bayesian models have a higher standard deviation, partly because there is an intrinsic randomness in the sampling mechanism, and it can be the cause of the occasional worse performance. In relation to this, we observe that the methods that use the trimmed mean as a summary statistic tend to have a worse score, as this statistic is more sensitive to outliers than the median or the mode.

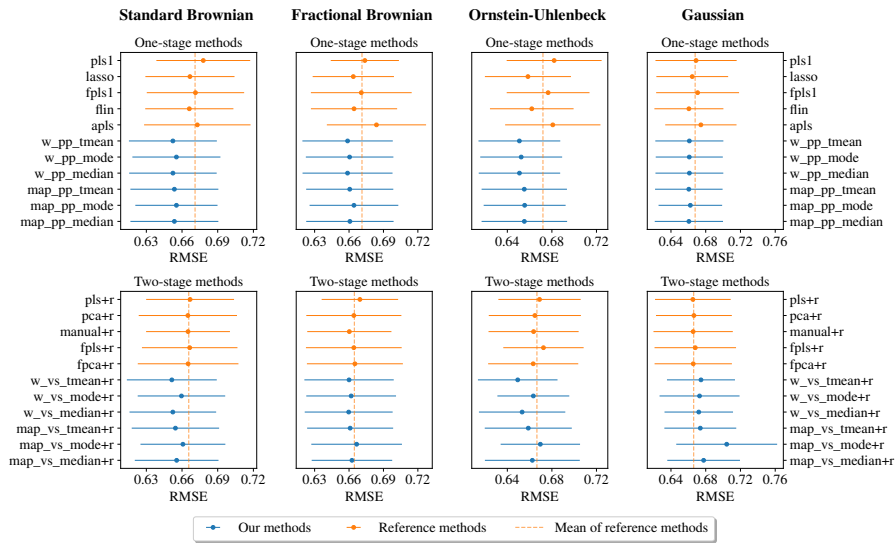


Figure 2: Mean and standard error of RMSE of predictors (lower is better) for 10 runs with GP regressors, one on each column, that obey an underlying linear L^2 -model.

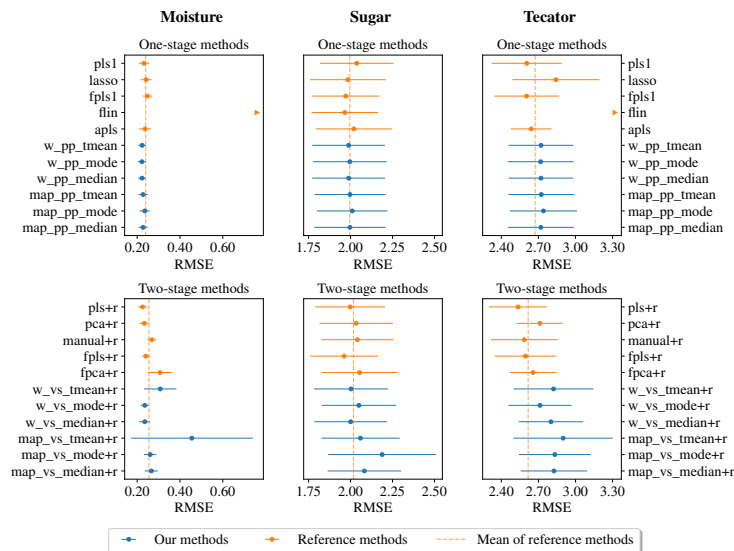


Figure 3: Mean and standard error of RMSE of predictors (lower is better) for 10 runs with real data sets, one on each column.

4.2 Functional logistic regression

In this case we set the same prior distribution for p as in the linear case, but now in the fitting phase the regressors are scaled to have standard deviation 0.5 to accommodate the priors in (2.6). We use the standard threshold of 0.5 to convert probabilities to class labels, and the performance metric is the accuracy, i.e., the rate of correctly predicted samples.

Simulated data sets

First, in Figure 4 we see the results for the GP regressors with a logistic RKHS response. Our models perform fairly well in this advantageous situation, and even more so in the one-stage case. We again improve the results of other models that can select far more components than our self-imposed limit of 10. Moreover, whenever our two-stage methods score lower, the differences account for only a couple of misclassified samples at worst.

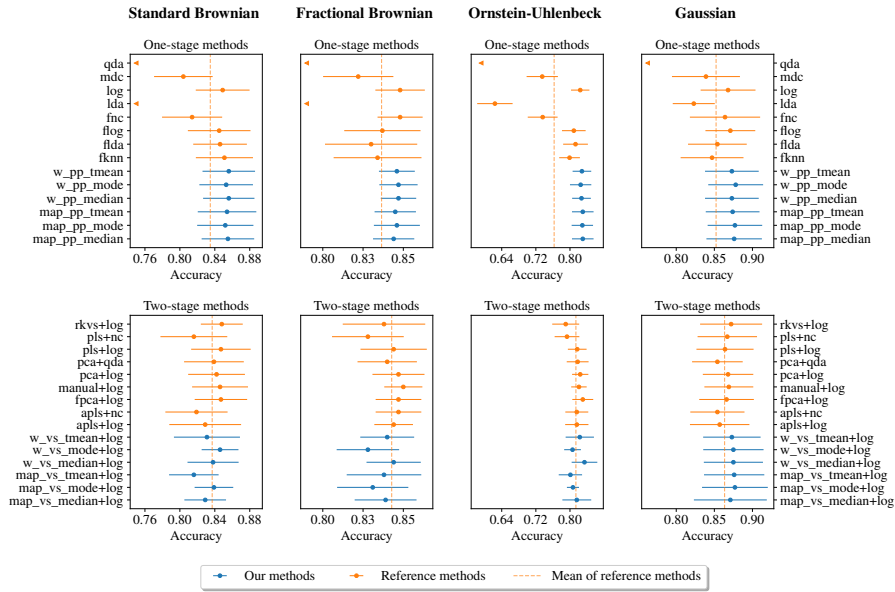


Figure 4: Mean and standard error of accuracy of classifiers (higher is better) for 10 runs with GP regressors, one on each column, that obey an underlying logistic RKHS model.

Subsequently, Figure 5 shows that in the L^2 scenario the results are again promising, since our models score consistently on or above the mean of the reference models, and in many instances surpass most of them. In this case we also beat the alternative functional logistic regression method (*flog*). In addition, in this situation the overall accuracy of all methods is poor (around 60%), so this is indeed a difficult problem in which even small increases in accuracy are relevant.

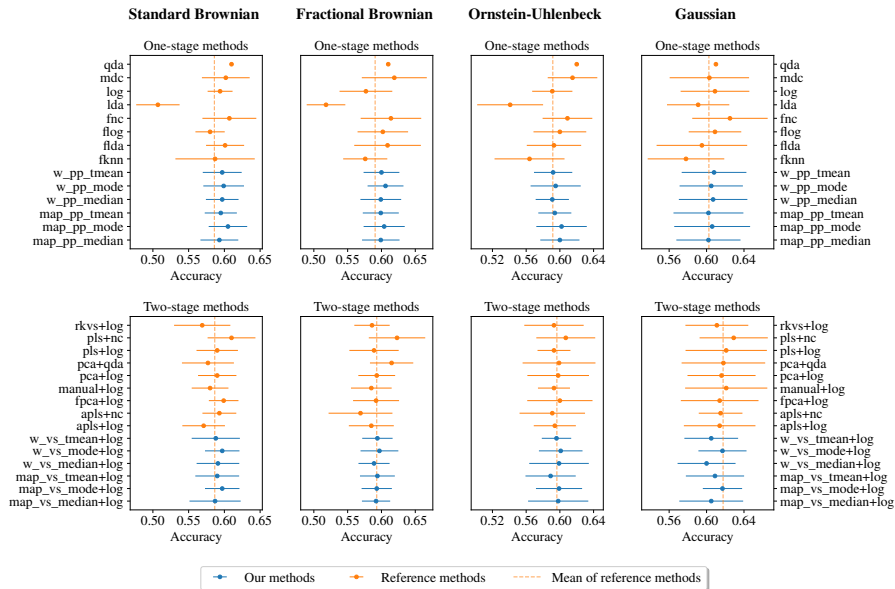


Figure 5: Mean and standard error of accuracy of classifiers (higher is better) for 10 runs with GP regressors, one on each column, that obey an underlying logistic L^2 -model.

Real data

As for the real data sets, in Figure 6 we see positive results in general, obtaining in some cases accuracies well above the mean of the reference models. In particular, the weighted sum methods tend to have slightly better

results than the MAP methods, which is a trend that was also present in the simulated data sets. This was somewhat expected, since the weighted predictions use the full range of information available.

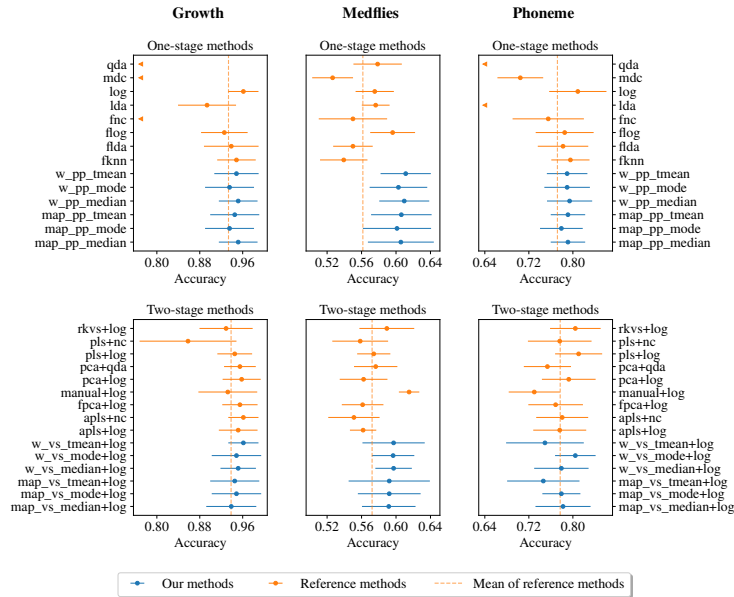


Figure 6: Mean and standard error of accuracy of classifiers (higher is better) for 10 runs with real data sets, one on each column.

5 Conclusion

In this work we have introduced a natural and computationally feasible way of integrating Bayesian inference into functional regression models, by means of a RKHS approach that simplifies the usually hard task of setting a prior distribution on a functional space. The proposed RKHS formulation gives a common framework to all finite-dimensional models based on linear combinations of the marginals of the underlying process, establishing a solid theoretical foundation for these popular models while retaining the functional perspective. Our approximation has the advantage of working with simpler functional parameters, thus increasing the interpretability and ease of implementation, as well as allowing direct comparison of models with different dimension. In addition, this approach works especially well in the logistic case, bypassing the difficulties associated with maximum likelihood techniques and providing a tractable alternative to the more studied methods in the literature.

We have also proved a posterior consistency result that ensures the coherence and correctness of the Bayesian methods we developed. These kinds of results have in other contexts more intricate and restrictive conditions to arrive at essentially the same conclusions as we did, but again the introduction of RKHS's is the key point to greatly simplifying them. It is worth emphasizing that the methodology introduced in Miller (2023), initially intended for mixtures, can be adapted to a completely different scenario to deal with functional data, giving a positive answer to a problem outside the usual scope of application of Doob's results.

Lastly, we have presented numerical evidence that supports the proposed Bayesian methodology and its predictive performance with simulated and real data sets. Thanks to our RKHS formulation, we can effectively leverage the capabilities of RJMCMC samplers and integrate the unknown number of components p in the Bayesian procedure, which to our knowledge is a novel application in the FDA context. This practical side of our work goes to show that the prediction methods we constructed from the posterior distribution are competitive against several non-cherry-picked frequentist techniques, especially those based on the usual L^2 -models, while still remaining viable implementation-wise. Of course, we are not suggesting that the L^2 perspective should be abandoned, but merely offering a simple, theoretically-backed alternative that can perform better in many situations.

Acknowledgments

The authors would like to acknowledge the computational resources provided by the Centro de Computación Científica-Universidad Autónoma de Madrid (CCC-UAM). This research was partially supported by grants PID2019-109387GB-I00 and PRE2020-095147 of the Spanish Ministry of Science and Innovation (MCIN), co-financed by the European Social Fund (ESF). J. R. Berrendero and A. Cuevas also acknowledge financial support from grant CEX2019-000904-S funded by MCIN/AEI/10.13039/501100011033.

References

- Abdi, H. (2010). “Partial least squares regression and projection on latent structure regression (PLS Regression).” *WIREs Computational Statistics*, 2(1): 97–106. doi: <https://doi.org/10.1002/wics.5128>
- Abraham, C. (2024). “An informative prior distribution on functions with application to functional regression.” *Statistica Neerlandica*, 78(2): 357–373. doi: <https://doi.org/10.1111/stan.12322>. 3
- Abraham, C. and Grollemund, P.-M. (2020). “Posterior concentration for a misspecified Bayesian regression model with functional covariates.” *Journal of Statistical Planning and Inference*, 208: 58–65. doi: <https://doi.org/10.1016/j.jspi.2020.01.008>. 2
- Aguilera, A. M. and Aguilera-Morillo, M. (2013). “Comparative study of different B-spline approaches for functional data.” *Mathematical and Computer Modelling*, 58(7-8): 1568–1579. doi: <https://doi.org/10.1016/j.mcm.2013.04.007>. 2
- Aguilera, A. M., Escabias, M., Preda, C., and Saporta, G. (2010). “Using basis expansions for estimating functional PLS regression: applications with chemometric data.” *Chemometrics and Intelligent Laboratory Systems*, 104(2): 289–305. doi: <https://doi.org/10.1016/j.chemolab.2010.09.007>. 28
- Albert, A. and Anderson, J. A. (1984). “On the existence of maximum likelihood estimates in logistic regression models.” *Biometrika*, 71(1): 1–10. doi: <https://doi.org/10.1093/biomet/71.1.1>. 6
- Amewou-Atisso, M., Ghosal, S., Ghosh, J. K., and Ramamoorthi, R. V. (2003). “Posterior consistency for semi-parametric regression problems.” *Bernoulli*, 9(2): 291–312. doi: <https://doi.org/10.3150/bj/1068128979>. 2
- Berlinet, A. and Thomas-Agnan, C. (2004). *Reproducing Kernel Hilbert Spaces in Probability and Statistics*. Springer. doi: <https://doi.org/10.1007/978-1-4419-9096-9>. 3
- Berrendero, J. R., Bueno-Larraz, B., and Cuevas, A. (2019). “An RKHS model for variable selection in functional linear regression.” *Journal of Multivariate Analysis*, 170: 25–45. doi: <https://doi.org/10.1016/j.jmva.2018.04.008>. 3, 5
- (2020). “On Mahalanobis Distance in Functional Settings.” *Journal of Machine Learning Research*, 21(9): 1–33. url: <http://jmlr.org/papers/v21/18-156.html>. 2
- (2023). “On functional logistic regression: some conceptual issues.” *Test*, 32: 321–349. doi: <https://doi.org/10.1007/s11749-022-00836-9>. 3, 6, 28
- Berrendero, J. R., Cholaquidis, A., and Cuevas, A. (2024). “On the functional regression model and its finite-dimensional approximations.” *Statistical Papers*, 1–35. doi: <https://doi.org/10.1007/s00362-024-01567-9>. 3, 5
- Berrendero, J. R., Cuevas, A., and Torrecilla, J. L. (2016). “Variable selection in functional data classification: a maxima-hunting proposal.” *Statistica Sinica*, 619–638. doi: <https://doi.org/10.5705/ss.202014.0014>. 3
- (2018). “On the use of reproducing kernel Hilbert spaces in functional classification.” *Journal of the American Statistical Association*, 113(523): 1210–1218. doi: <https://doi.org/10.1080/01621459.2017.1320287>. 2, 6, 28
- Borggaard, C. and Thodberg, H. H. (1992). “Optimal minimal neural interpretation of spectra.” *Analytical Chemistry*, 64(5): 545–551. doi: <https://doi.org/10.1021/ac00029a018>. 13
- Bro, R. (1999). “Exploratory study of sugar production using fluorescence spectroscopy and multi-way analysis.” *Chemometrics and Intelligent Laboratory Systems*, 46(2): 133–147. doi: [https://doi.org/10.1016/s0169-7439\(98\)00181-6](https://doi.org/10.1016/s0169-7439(98)00181-6). 13

- Brooks, S. P., Giudici, P., and Roberts, G. O. (2003). “Efficient construction of reversible jump Markov chain Monte Carlo proposal distributions.” *Journal of the Royal Statistical Society Series B: Statistical Methodology*, 65(1): 3–39. doi: <https://doi.org/10.1111/1467-9868.03711>. 7
- Bueno-Larraz, B. and Klepsch, J. (2019). “Variable Selection for the Prediction of $C[0, 1]$ -Valued Autoregressive Processes using Reproducing Kernel Hilbert Spaces.” *Technometrics*, 61(2): 139–153. doi: <https://doi.org/10.1080/00401706.2018.1505660>. 3
- Candès, E. J. and Sur, P. (2020). “The phase transition for the existence of the maximum likelihood estimate in high-dimensional logistic regression.” *The Annals of Statistics*, 48(1): 27 – 42. doi: <https://doi.org/10.1214/18-AOS1789>. 6
- Cardot, H. and Sarda, P. (2018). “Functional Linear Regression.” In Ferraty, F. and Romain, Y. (eds.), *The Oxford Handbook of Functional Data Analysis*, 21–46. Oxford Handbooks. doi: <https://doi.org/10.1093/oxfordhb/9780199568444.013.2>. 3
- Carey, J. R., Liedo, P., Müller, H.-G., Wang, J.-L., and Chiou, J.-M. (1998). “Relationship of Age Patterns of Fecundity to Mortality, Longevity, and Lifetime Reproduction in a Large Cohort of Mediterranean Fruit Fly Females.” *The Journals of Gerontology: Series A*, 53(4): B245–B251. doi: <https://doi.org/10.1093/gerona/53a.4.b245>. 13
- Carlin, B. P. and Chib, S. (1995). “Bayesian model choice via Markov chain Monte Carlo methods.” *Journal Of The Royal Statistical Society Series B: Statistical Methodology*, 57(3): 473–484. doi: <https://doi.org/10.1111/j.2517-6161.1995.tb02042.x>. 5
- Celeux, G., Hurn, M., and Robert, C. P. (2000). “Computational and Inferential Difficulties with Mixture Posterior Distributions.” *Journal of the American Statistical Association*, 95(451): 957–970. doi: <https://doi.org/10.1080/01621459.2000.10474285>. 23
- Choi, T. and Ramamoorthi, R. V. (2008). “Remarks on consistency of posterior distributions.” In Clarke, B. and Ghosal, S. (eds.), *Pushing the limits of contemporary statistics: contributions in honor of Jayanta K. Ghosh*, 170–186. Institute of Mathematical Statistics Collections. doi: <https://doi.org/10.1214/074921708000000138>. 2, 9
- Crainiceanu, C. M. and Goldsmith, A. J. (2010). “Bayesian Functional Data Analysis Using WinBUGS.” *Journal of Statistical Software*, 32(11): 1–33. doi: <https://doi.org/10.18637/jss.v032.i11>. 2
- Cuevas, A. (2014). “A partial overview of the theory of statistics with functional data.” *Journal of Statistical Planning and Inference*, 147: 1–23. doi: <https://doi.org/10.1016/j.jspi.2013.04.002>. 1
- Cuevas, A., Febrero, M., and Fraiman, R. (2004). “An anova test for functional data.” *Computational Statistics & Data Analysis*, 47(1): 111–122. doi: <https://doi.org/10.1016/j.csda.2003.10.021>. 2
- Davies, L., Salomone, R., Sutton, M., and Drovandi, C. (2023). “Transport Reversible Jump Proposals.” In Ruiz, F., Dy, J., and van de Meent, J.-W. (eds.), *Proceedings of The 26th International Conference on Artificial Intelligence and Statistics*, volume 206 of *Proceedings of Machine Learning Research*, 6839–6852. PMLR. url: <https://proceedings.mlr.press/v206/davies23a.html>. 7
- Delaique, A. and Hall, P. (2012a). “Achieving near Perfect Classification for Functional Data.” *Journal of the Royal Statistical Society Series B: Statistical Methodology*, 74(2): 267–286. doi: <https://doi.org/10.1111/j.1467-9868.2011.01003.x>. 6, 28
- (2012b). “Methodology and theory for partial least squares applied to functional data.” *The Annals of Statistics*, 40(1): 322–352. doi: <https://doi.org/10.1214/11-aos958>. 28
- Diaconis, P. and Freedman, D. (1986). “On the Consistency of Bayes Estimates.” *The Annals of Statistics*, 14(1): 1–26. doi: <https://doi.org/10.1214/aos/1176349830>. 10
- Doob, J. L. (1949). “Application of the theory of martingales.” *Le calcul des probabilités et ses applications. Colloques Internationaux*, 13: 23–27. url: <https://www.jehps.net/juin2009/Locker.pdf> [at the end]. 8
- Dudley, R. M. (2002). *Real Analysis and Probability*. Cambridge University Press. doi: <https://doi.org/10.1017/CB09780511755347>. 27
- Ferguson, T. S. (1974). “Prior Distributions on Spaces of Probability Measures.” *The Annals of Statistics*, 2(4): 615 – 629. doi: <https://doi.org/10.1214/aos/1176342752>. 2
- Ferraty, F., Hall, P., and Vieu, P. (2010). “Most-predictive design points for functional data predictors.” *Biometrika*, 97(4): 807–824. doi: <https://doi.org/10.1093/biomet/asq058>. 3
- Folland, G. B. (1999). *Real Analysis: Modern Techniques and Their Applications*. John Wiley & Sons. 27

- Foreman-Mackey, D., Hogg, D. W., Lang, D., and Goodman, J. (2013). “emcee: the MCMC hammer.” *Publications of the Astronomical Society of the Pacific*, 125(925): 306–312. doi: <https://doi.org/10.1086/670067>. 24
- Galeano, P., Joseph, E., and Lillo, R. E. (2015). “The Mahalanobis Distance for Functional Data With Applications to Classification.” *Technometrics*, 57(2): 281–291. doi: <https://doi.org/10.1080/00401706.2014.902774>. 2
- Gelman, A., Jakulin, A., Pittau, M. G., and Su, Y.-S. (2008). “A weakly informative default prior distribution for logistic and other regression models.” *The Annals of Applied Statistics*, 2(4): 1360–1383. doi: <https://doi.org/10.1214/08-AOAS191>. 6
- Gelman, A. and Rubin, D. B. (1992). “Inference from iterative simulation using multiple sequences.” *Statistical Science*, 7(4): 457–472. doi: <https://doi.org/10.1214/ss/1177011136>. 31
- Ghosh, A. K. and Chaudhuri, P. (2005). “On Maximum Depth and Related Classifiers.” *Scandinavian Journal of Statistics*, 32(2): 327–350. doi: <https://doi.org/10.1111/j.1467-9469.2005.00423.x>. 28
- Ghosh, J., Li, Y., and Mitra, R. (2018). “On the use of Cauchy prior distributions for Bayesian logistic regression.” *Bayesian Analysis*, 13(2): 359–383. doi: <https://doi.org/10.1214/17-BA1051>. 6
- Ghosh, J. and Ramamoorthi, R. V. (2003). *Bayesian Nonparametrics*. Springer. doi: <https://doi.org/10.1007/b97842>. 8, 9
- Goia, A. and Vieu, P. (2016). “An introduction to recent advances in high/infinite dimensional statistics.” *Journal of Multivariate Analysis*, 146: 1–6. doi: <https://doi.org/10.1016/j.jmva.2015.12.001>. 1
- Goodman, J. and Weare, J. (2010). “Ensemble samplers with affine invariance.” *Communications in Applied Mathematics and Computational Science*, 5(1): 65–80. doi: <https://doi.org/10.2140/camcos.2010.5.65>. 24
- Green, P. J. (1995). “Reversible jump Markov chain Monte Carlo computation and Bayesian model determination.” *Biometrika*, 82(4): 711–732. doi: <https://doi.org/10.2307/2337340>. 2, 7
- Grollemund, P.-M., Abraham, C., Baragatti, M., and Pudlo, P. (2019). “Bayesian Functional Linear Regression with Sparse Step Functions.” *Bayesian Analysis*, 14(1): 111 – 135. doi: <https://doi.org/10.1214/18-BA1095>. 3, 5
- Hastie, T., Buja, A., and Tibshirani, R. (1995). “Penalized discriminant analysis.” *The Annals of Statistics*, 23(1): 73–102. doi: <https://doi.org/10.1214/aos/1176324456>. 13
- Hoeting, J. A., Madigan, D., Raftery, A. E., and Volinsky, C. T. (1999). “Bayesian model averaging: a tutorial (with comments by M. Clyde, David Draper and E. I. George, and a rejoinder by the authors).” *Statistical Science*, 14(4): 382–417. doi: <https://doi.org/10.1214/ss/1009212519>. 5
- Hsing, T. and Eubank, R. (2015). *Theoretical Foundations of Functional Data Analysis, with an Introduction to Linear Operators*. John Wiley & Sons. doi: <https://doi.org/10.1002/9781118762547>. 1
- Hukushima, K. and Nemoto, K. (1996). “Exchange Monte Carlo method and application to spin glass simulations.” *Journal of the Physical Society of Japan*, 65(6): 1604–1608. doi: <https://doi.org/10.1143/JPSJ.65.1604>. 12
- Jasra, A., Holmes, C. C., and Stephens, D. A. (2005). “Markov Chain Monte Carlo Methods and the Label Switching Problem in Bayesian Mixture Modeling.” *Statistical Science*, 20(1): 50–67. doi: <https://doi.org/10.1214/088342305000000016>. 24
- Jeffreys, H. (1946). “An invariant form for the prior probability in estimation problems.” *Proceedings of the Royal Society of London Series A: Mathematical and Physical Sciences*, 186(1007): 453–461. doi: <https://doi.org/10.1098/rspa.1946.0056>. 5
- Kalivas, J. H. (1997). “Two data sets of near infrared spectra.” *Chemometrics and Intelligent Laboratory Systems*, 37(2): 255–259. doi: [https://doi.org/10.1016/s0169-7439\(97\)00038-5](https://doi.org/10.1016/s0169-7439(97)00038-5). 13
- Karnesis, N., Katz, M. L., Korsakova, N., Gair, J. R., and Stergioulas, N. (2023). “Eryn: a multipurpose sampler for Bayesian inference.” *Monthly Notices of the Royal Astronomical Society*, 526(4): 4814–4830. doi: <https://doi.org/10.1093/mnras/stad2939>. 12, 25, 26
- Korsakova, N., Babak, S., Katz, M. L., Karnesis, N., Khukhlaev, S., and Gair, J. R. (2024). “Neural density estimation for Galactic Binaries in LISA data analysis.” *arXiv preprint arXiv:2402.13701*. 7

- Kupresanin, A., Shin, H., King, D., and Eubank, R. (2010). “An RKHS framework for functional data analysis.” *Journal of Statistical Planning and Inference*, 140(12): 3627–3637. doi: <https://doi.org/10.1016/j.jspi.2010.04.030>. 2
- Lian, H., Choi, T., Meng, J., and Jo, S. (2016). “Posterior convergence for Bayesian functional linear regression.” *Journal of Multivariate Analysis*, 150: 27–41. doi: <https://doi.org/10.1016/j.jmva.2016.04.008>. 2
- Loève, M. (1948). “Fonctions aléatoires du second ordre.” In Lévy, P. (ed.), *Processus stochastiques et mouvement Brownien*, 299–352. Gauthier-Villars. 4
- López-Pintado, S. and Romo, J. (2009). “On the Concept of Depth for Functional Data.” *Journal of the American Statistical Association*, 104(486): 718–734. doi: <https://doi.org/10.1198/jasa.2009.0108>. 2
- Lukić, M. N. and Beder, J. H. (2001). “Stochastic processes with sample paths in reproducing kernel Hilbert spaces.” *Transactions of the American Mathematical Society*, 353(10): 3945–3969. doi: <https://doi.org/10.1090/s0002-9947-01-02852-5>. 4
- Miller, J. W. (2023). “Consistency of mixture models with a prior on the number of components.” *Dependence Modeling*, 11(1): 20220150. doi: <https://doi.org/10.1515/demo-2022-0150>. 9, 10, 11, 12, 17
- Miller, J. W. and Harrison, M. T. (2018). “Mixture Models with a Prior on the Number of Components.” *Journal of the American Statistical Association*, 113(521): 340–356. doi: <https://doi.org/10.1080/01621459.2016.1255636>. 10
- Müller, H.-G. and Stadtmüller, U. (2005). “Generalized functional linear models.” *The Annals of Statistics*, 33(2): 774–805. doi: <https://doi.org/10.1214/009053604000001156>. 2
- Nobile, A. (1994). “Bayesian analysis of finite mixture distributions.” Ph.D. thesis, Carnegie Mellon University. 10, 12
- Nobile, A. and Fearnside, A. T. (2007). “Bayesian finite mixtures with an unknown number of components: The allocation sampler.” *Statistics and Computing*, 17: 147–162. doi: <https://doi.org/10.1007/s11222-006-9014-7>. 13
- Parzen, E. (1961). “An Approach to Time Series Analysis.” *The Annals of Mathematical Statistics*, 32(4): 951–989. doi: <https://doi.org/10.1214/aoms/1177704840>. 4
- Pedregosa, F., Varoquaux, G., Gramfort, A., Michel, V., Thirion, B., Grisel, O., Blondel, M., Prettenhofer, P., Weiss, R., Dubourg, V., Vanderplas, J., Passos, A., Cournapeau, D., Brucher, M., Perrot, M., and Duchesnay, É. (2011). “Scikit-learn: Machine Learning in Python.” *Journal of Machine Learning Research*, 12(85): 2825–2830. url: <http://jmlr.org/papers/v12/pedregosa11a.html>. 29
- Preda, C., Saporta, G., and Lévêder, C. (2007). “PLS classification of functional data.” *Computational Statistics*, 22(2): 223–235. doi: <https://doi.org/10.1007/s00180-007-0041-4>. 28
- Ramos-Carreño, C., Torrecilla, J. L., Carbajo-Berrocal, M., Marcos, P., and Suárez, A. (2024). “scikit-fda: A Python Package for Functional Data Analysis.” *Journal of Statistical Software*, 109(2): 1–37. doi: <https://doi.org/10.18637/jss.v109.i02>. 29
- Ramsay, J. O. and Silverman, B. W. (2005). *Functional Data Analysis*. Springer. doi: <https://doi.org/10.1007/b98888>. 2
- Reiss, P. T., Goldsmith, J., Shang, H. L., and Ogden, R. T. (2017). “Methods for Scalar-on-Function Regression.” *International Statistical Review*, 85(2): 228–249. doi: <https://doi.org/10.1111/insr.12163>. 3
- Richardson, S. and Green, P. J. (1997). “On Bayesian analysis of mixtures with an unknown number of components (with discussion).” *Journal of the Royal Statistical Society Series B: Statistical Methodology*, 59(4): 731–792. doi: <https://doi.org/10.1111/1467-9868.00095>. 7
- Robert, C. P. (2014). “On the Jeffreys-Lindley paradox.” *Philosophy of Science*, 81(2): 216–232. doi: <https://doi.org/10.1086/675729>. 5
- Rodríguez, C. E. and Walker, S. G. (2014). “Label Switching in Bayesian Mixture Models: Deterministic Relabeling Strategies.” *Journal of Computational and Graphical Statistics*, 23(1): 25–45. doi: <https://doi.org/10.1080/10618600.2012.735624>. 24
- Roodaki, A., Bect, J., and Fleury, G. (2014). “Relabeling and Summarizing Posterior Distributions in Signal Decomposition Problems When the Number of Components is Unknown.” *IEEE Transactions On Signal Processing*, 62(16): 4091–4104. doi: <https://doi.org/10.1109/TSP.2014.2333569>. 23

- Rosenthal, J. S. (2011). “Optimal proposal distributions and adaptive MCMC.” In Brooks, S., Gelman, A., Jones, G., and Meng, X.-L. (eds.), *Handbook of Markov Chain Monte Carlo*, 93–111. Chapman & Hall/CRC. doi: <https://doi.org/10.1201/b10905>. 26
- Schwartz, L. (1965). “On Bayes procedures.” *Zeitschrift für Wahrscheinlichkeitstheorie und Verwandte Gebiete*, 4(1): 10–26. doi: <https://doi.org/10.1007/bf00535479>. 9
- Shi, J. Q. and Choi, T. (2011). *Gaussian Process Regression Analysis for Functional Data*. Chapman and Hall/CRC. doi: <https://doi.org/10.1201/b11038>. 2
- Shin, H. (2008). “An extension of Fisher’s discriminant analysis for stochastic processes.” *Journal of Multivariate Analysis*, 99(6): 1191–1216. doi: <https://doi.org/10.1016/j.jmva.2007.08.001>. 2
- Simola, U., Cisewski-Kehe, J., and Wolpert, R. L. (2021). “Approximate Bayesian computation for finite mixture models.” *Journal of Statistical Computation and Simulation*, 91(6): 1155–1174. doi: <https://doi.org/10.1080/00949655.2020.1843169>. 24
- Sperrin, M., Jaki, T., and Wit, E. (2010). “Probabilistic relabelling strategies for the label switching problem in Bayesian mixture models.” *Statistics and Computing*, 20: 357–366. doi: <https://doi.org/10.1007/s11222-009-9129-8>. 24
- Stephens, M. (2000). “Dealing With Label Switching in Mixture Models.” *Journal of the Royal Statistical Society Series B: Statistical Methodology*, 62(4): 795–809. doi: <https://doi.org/10.1111/1467-9868.00265>. 12, 23
- Torrecilla, J. L., Ramos-Carreño, C., Sánchez-Montañés, M., and Suárez, A. (2020). “Optimal classification of Gaussian processes in homo- and heteroscedastic settings.” *Statistics and Computing*, 30(4): 1091–1111. doi: <https://doi.org/10.1007/s11222-020-09937-7>. 6, 29
- Tuddenham, R. D. and Snyder, M. M. (1954). “Physical growth of California boys and girls from birth to eighteen years.” *University of California Publications in Child Development*, 1(2): 183–364. url: <https://pubmed.ncbi.nlm.nih.gov/13217130/>. 13
- Ullah, S. and Finch, C. F. (2013). “Applications of functional data analysis: A systematic review.” *BMC Medical Research Methodology*, 13:43: 1–12. doi: <https://doi.org/10.1186/1471-2288-13-43>. 1
- Yuan, M. and Cai, T. T. (2010). “A reproducing kernel Hilbert space approach to functional linear regression.” *The Annals of Statistics*, 38(6): 3412–3444. doi: <https://doi.org/10.1214/09-AOS772>. 2

A Model choice and implementation details

A.1 Posterior distributions

For the posterior distributions in our Bayesian formulation, we only compute a function proportional to their log-density, since that is enough for a MCMC algorithm to work. Consider the parameter vector (p, θ_p) , where $\theta_p = (b_p, \tau_p, \alpha_0, \sigma^2)$ with $b_p = (\beta_1, \dots, \beta_p)$ and $\tau_p = (t_1, \dots, t_p)$. Recall that we have a labeled data set of independent observations from (X, Y) , denoted by $\mathcal{D}_n = \{(X_i, Y_i) : i = 1, \dots, n\}$. A standard algebraic manipulation in the posterior expression using Bayes' formula yields the following results.

Proposition 6. *Under the linear RKHS model and the prior distribution in Section 2.1, the log-posterior distribution up to an additive constant is*

$$\begin{aligned} \log \pi(p, \theta_p \mid \mathcal{D}_n) \propto & -\frac{1}{2} \left(\frac{\|b_p\|^2}{\eta^2} - \frac{\|\mathbf{Y} - \alpha_0 \mathbf{1} + \mathcal{X}_{\tau_p} b_p\|^2}{\sigma^2} \right) - (n+2) \log \sigma \\ & - p \log \eta - \frac{p}{2} \log(2\pi) + \log \pi(p), \end{aligned}$$

where $\mathbf{Y} = (Y_1, \dots, Y_n)^T$, $\mathbf{1}$ is an n -dimensional vector of ones, and \mathcal{X}_{τ_p} is the data matrix $(X_i(t_j))_{i,j}$, for $i = 1, \dots, n$ and $j = 1, \dots, p$.

Proposition 7. *Under the logistic RKHS model and the prior distribution in Section 2.2, the log-posterior distribution up to an additive constant is*

$$\begin{aligned} \log \pi(p, \theta_p \mid \mathcal{D}_n) \propto & \sum_{i=1}^n [Y_i (\alpha_0 + \langle X_i, \alpha \rangle_K) - \log(1 + \exp\{\alpha_0 + \langle X_i, \alpha \rangle_K\})] \\ & - 3 \sum_{j=1}^p \log(4\beta_j^2 + 125) + p \left[\frac{15}{2} \log 5 + 4 \log 2 - \log(3\pi) \right] \\ & - \log(100 + \alpha_0^2) + \log \pi(p), \end{aligned}$$

where $\langle X_i, \alpha \rangle_K = \sum_{j=1}^p \beta_j X_i(t_j)$.

The discrete distribution $\pi(p)$ used in the experiments is either uniform in $\{1, \dots, 10\}$, with density $\pi_{\text{uniform}}(p) = 1/10$, or a Poisson distribution with rate parameter $\lambda = 3$ truncated to $\{1, \dots, 10\}$, with density

$$\pi_{\text{Poisson}}(p) = \frac{3^p}{C p!}, \quad p \in \{1, \dots, 10\},$$

where the normalization constant is $C = \sum_{k=1}^{10} \frac{3^k}{k!}$.

A.2 Label switching

A well-known issue that arises when using MCMC methods in mixture-like models such as the one proposed in this work is *label switching*, which in short refers to the non-identifiability of the components of the model caused by their interchangeability. In our case, this happens because the likelihood and the prior are symmetric with respect to the ordering of the parameters b and τ , i.e., $\pi(Y|X, \theta) = \pi(Y|X, \nu(\theta))$ for any permutation ν that rearranges the indices $j = 1, \dots, p$. Thus, since the components are arbitrarily ordered, they may be inadvertently exchanged from one iteration to the next in a MCMC algorithm. This can cause nonsensical answers when summarizing the marginal posterior distributions of the parameters to perform inference, as different labelings might be mixed on each component (Stephens, 2000). This is primarily the reason why we do not directly use summaries of the posterior distribution of the individual parameters in our prediction methods.

Moreover, the use of trans-dimensional samplers exacerbates this problem, since the change in dimension can further disrupt the internal ordering of the components (see Roodaki et al., 2014). However, this phenomenon is perhaps surprisingly a condition for the convergence of the MCMC method: as pointed out by many authors (e.g. Celeux et al., 2000), a lack of switching would indicate that not all modes of the posterior distribution were being explored by the sampler. For this reason, many ad-hoc solutions revolve around post-processing and relabeling the samples to eliminate the switching effect, but they generally do not prevent it from happening in the first place.

The most straightforward solutions consist on imposing an artificial identifiability constraint on the parameters to break the symmetry of their posterior distributions; see Jasra et al. (2005) and references therein. A common approach that seems to work well is to simply enforce an ordering in the parameters in question, which in our case would mean requiring for example that $\beta_i < \beta_j$ for $i < j$, or the analogous with the times in τ . We have implemented a variation of this method described in Simola et al. (2021), which works by post-processing the samples and relabeling the components to satisfy the order constraint mentioned above, choosing either b or τ depending on which set of ordered parameters would produce the largest separation between any two of them (suitably averaged across all iterations of the chains). This is an area of ongoing research, and thus there are other, more complex relabeling strategies, both deterministic and probabilistic. A summary of several such methods can be found for example in Sperrin et al. (2010) or Rodríguez and Walker (2014).

A.3 Affine-invariant ensemble samplers

An interesting and often desirable property of regular MCMC sampling algorithms is that they be *affine-invariant*, which informally means that they regard two distributions that differ in an affine transformation, say $\pi(x)$ and $\pi_{A,b}(Ax + b)$, as equally difficult to sample from. This is useful when one is working with very asymmetrical or skewed distributions, for an affine transformation can turn them into ones with simpler shapes. Generally speaking, a MCMC algorithm can be described through a function R as $\Lambda(t+1) = R(\Lambda(t), \xi(t), \pi)$, where $\Lambda(t)$ is the state of the chain at instant t , π is the objective distribution, and $\xi(t)$ is a sequence of i.i.d. random variables that represent the random behavior of the chain. With this notation, the affine-invariance property can be characterized as $R(A\lambda + b, \xi(t), \pi_{A,b}) = AR(\lambda, \xi(t), \pi) + b$, for all A, b and λ , and almost all $\xi(t)$. This means that if we fix a random generator and run the algorithm twice, one time using π and starting in $\Lambda(0)$ and a second time using $\pi_{A,b}$ with initial point $\Gamma(0) = A\Lambda(0) + b$, then $\Gamma(t) = A\Lambda(t) + b$ for all t . In Goodman and Weare (2010) the authors consider an ensemble of samplers with the affine invariance property. Specifically, they work with a set $\Lambda = (\Lambda_1, \dots, \Lambda_L)$ of *walkers*, where $\Lambda_l(t)$ represents an individual chain at time t . At each iteration, an affine-invariant transformation is used to find the next point, which is constructed using the current values of the rest of the walkers (similar to Gibb's algorithm), namely the *complementary ensemble*

$$\Lambda_{-l}(t) = \{\Lambda_1(t+1), \dots, \Lambda_{l-1}(t+1), \Lambda_{l+1}(t), \dots, \Lambda_L(t)\}, \quad l = 1, \dots, L.$$

To maintain the affine invariance and the joint distribution of the ensemble, the walkers are advanced one by one following a Metropolis-Hastings acceptance scheme. The authors consider mainly two types of moves.

Stretch move. For each walker $1 \leq l \leq L$ another walker $\Lambda_j \in \Lambda_{-l}(t)$ is chosen at random, and the proposal is constructed as

$$\Lambda_l(t) \rightarrow \Gamma = \Lambda_j + Z(\Lambda_l(t) - \Lambda_j),$$

where $Z \stackrel{i.i.d.}{\sim} g(z)$ satisfying the symmetry condition $g(z^{-1}) = zg(z)$. In particular, the suggested density is

$$g_a(z) \propto \begin{cases} \frac{1}{\sqrt{z}}, & \text{if } z \in [a^{-1}, a], \\ 0, & \text{otherwise.} \end{cases}, \quad a > 1.$$

Supposing \mathbb{R}^p is the sample space, the corresponding acceptance probability (chosen so that the detailed balance equations are satisfied) is:

$$\alpha = \min \left\{ 1, Z^{p-1} \frac{\pi(\Gamma)}{\pi(\Lambda_l(t))} \right\}.$$

Walk move. For each walker $1 \leq l \leq L$ a random subset $S_l \subseteq \Lambda_{-l}(t)$ with $|S_l| \geq 2$ is selected, and the proposed move is

$$\Lambda_l(t) \rightarrow \Gamma = \Lambda_l(t) + W,$$

where W is a normal distribution with mean 0 and the same covariance as the sample covariance of all walkers in S_l . The acceptance probability in this case is just the Metropolis ratio, namely $\alpha = \min\{1, \pi(\Gamma)/\pi(\Lambda_l(t))\}$.

From a computational perspective, the Python library *emcee* (Foreman-Mackey et al., 2013) provides a parallel implementation of this algorithm. The idea is to divide the ensemble Λ into two equally-sized subsets $\Lambda^{(0)}$ and $\Lambda^{(1)}$, and then proceed on each iteration in the following alternate fashion:

1. Update *all* walkers in $\Lambda^{(0)}$ through one of the available moves explained above, using $\Lambda^{(1)}$ as the complementary ensemble.
2. Use the new values in $\Lambda^{(0)}$ to update $\Lambda^{(1)}$.

In this way the detailed balance equations are still satisfied, and each of the steps can benefit from the computing power of an arbitrary number of processors (up to $L/2$).

A.4 RJMCMC implementation

For the computational implementation of our Bayesian prediction pipeline we chose the Python library *Eryn* (Karnesis et al., 2023). This package is a general-purpose suite of MCMC methods which is reliable, easy to use and performs well in a wide class of problems. It is an evolution of the *emcee* library mentioned in Appendix A.3 that implements affine-invariant ensemble samplers, with a few key improvements:

Reversible jump sampling. The main reason for choosing this library is that it implements a reversible jump MCMC sampling scheme, which is an essential element in our proposed models. It allows trans-dimensional sampling for posterior approximation, letting the user select the likelihood, prior and proposal distributions, and providing a great level of control over the details.

Parallel tempering. This is a mechanism to increase the efficiency with which the sampler explores the parameter space. The basic idea is to consider a set of Markov chains in parallel, each one sampling from a transformed posterior distribution $\pi_T(p, \theta_p | X, Y) = \pi(Y | X, p, \theta_p)^{1/T} \pi(p, \theta_p)$, where $T \geq 1$ is a temperature parameter. In the words of Karnesis et al. (2023), “intermediate temperatures ‘smooth out’ the posterior by reducing the contrast between areas of high and low likelihood”. In practice, these chains periodically exchange information, with the swaps controlled by an acceptance probability that maintains detailed balance, and ultimately we are only interested on the cold chain ($T = 1$).

Multiple try. Since the trans-dimensional moves are harder to manage and generally give a low acceptance rate, this library allows the proposal of several candidates for a given move, using a weight function to assign them a relative importance, and then choosing from them with probability given by the normalized weights. This naturally increases the computational cost, but it often produces better results.

Another advantage of this ensemble approach, apart from the property of affine-invariance, is that it only requires the specification of a few hyperparameters irrespective of the underlying dimension. This contrasts to, say, the $\mathcal{O}(N^2)$ degrees of freedom corresponding to the covariance matrix of an N -dimensional jump distribution in Metropolis-Hastings. We already covered the prior, likelihood and posterior distributions used in Section 2 and in Appendix A.1. We give below an overview of other integral parts of our RJMCMC method with some implementation details.

Initial values

We need to specify the initial values for the parameters of all the chains in our sampler. In general, we set these values by sampling from the prior distribution of the corresponding parameters. However, in the linear case the prior on (α_0, σ^2) is improper, so we use ad-hoc weakly informative distributions for the initial values instead. For α_0 we consider a normal distribution with mean 0 and standard deviation $10|\bar{Y}_{\text{scaled}}|$, where Y_{scaled} is the version of the original data scaled to have standard deviation unity. For σ^2 we use an inverse-gamma distribution with shape parameter $a = 2$ and scale parameter $b = \hat{\sigma}_Y^2 / \text{Var}(Y)$, where $\hat{\sigma}_Y^2$ is a rough estimate of an acceptable error in the scale of Y . This estimation is done in practice as two orders of magnitudes less than $|\bar{Y}|$.

Moves

As with any MCMC method, the Markov chains are advanced iteratively through a set of moves. For the *in-model* moves (that is, moves that do not change the dimension), we divide our parameter vector in two parts:

Stretch move. For the parameters α_0 and σ^2 , which are common to all sub-models, we use the stretch move explained in Appendix A.3.

Group stretch move. For b and τ , we use a variant of the stretch move known as the group stretch move, which was designed as an extension of the original move that can handle reversible jump setups. The

main difference is that the random walker Λ_j used to advance the chain is selected from a stationary group that does not change for several iterations (see Section 3.1 in Karnesis et al., 2023 for more information about this move).

In both moves above, the key scaling parameter a starts with a value of 2, and is changed dynamically to guide the sampler towards an acceptance rate of about 20% – 30%, which is within the range usually recommended in the literature (e.g. Rosenthal, 2011).

For the *between-model* moves (those which change the dimension), we set an equal probability of births and deaths, except on the end points of the range of p . Specifically, $b_{p,p+1} = d_{p,p-1} = 0.5$ if $1 < p < 10$, and $b_{1,2} = d_{10,9} = 1$. Note that these are only the probabilities to propose the corresponding move, which will be accepted or rejected according to the acceptance formula in Section 2.3. When the birth of a new component is proposed, we use the prior distribution of b and τ to generate the new values, and when a death is proposed, the method selects an existing component at random as a candidate for deletion.

Hyperparameters

Other relevant hyperparameters include the burn-in period for the chains, which is the number of initial samples discarded, the number of actual steps, the number of chains, and the number of temperatures for parallel tempering. In the experiments we use 64 chains and 10 different temperatures, and run them for 5000 iterations in total, discarding the first 4000 as burn-in. Moreover, when the prior on p is uniform (i.e. in the experiments with real data) we activate the multiple try scheme and set the number of tries to 2. Lastly, a computational decision we made is working with $\log \sigma$ instead of σ^2 so that the domain of this parameter is an unconstrained space, which is a widespread recommendation that helps increase the sampling efficiency.

B More details on posterior consistency

There are some technicalities to take into account in the theoretical exposition of posterior consistency in Section 3, especially pertaining to measure theory. For example, to justify the existence of regular conditional distributions such as $\theta|X_1, \dots, X_n$, one should see Theorem 10.2.1 and Theorem 10.2.2 in Dudley (2002), which guarantee they are well-defined provided that the underlying spaces are sufficiently regular. Another issue is the measurability of the mapping $\theta \mapsto P_\theta(X, Y)(A)$, which is assumed in the proof of our consistency results. We illustrate how this can be proved for example in the linear case, under the additional condition of sample continuity, which is arguably not a very restrictive condition in real-life scenarios.

Proposition 8. *If the process X is sample-continuous (i.e. the trajectories are continuous functions), then the mapping $\theta \mapsto P_\theta(X, Y)(A)$ is measurable for every measurable set $A \subseteq \mathcal{X} \times \mathcal{Y}$.*

Proof. We start by checking that $\theta \mapsto P_\theta(Y|X)(A_1)$ is measurable for every measurable set $A_1 \subseteq \mathcal{Y}$. Indeed, consider the function $F(y, \theta) = f(y|X, \theta)\mathbf{1}_{A_1}(y)$, where $f(\cdot|X, \theta)$ is the density of the normal distribution $\mathcal{N}(\alpha_0 + \sum_j \beta_j X(t_j), \sigma^2)$ and $\mathbf{1}_{A_1}$ is the indicator function of the set A_1 . It is easy to see that $F(y, \theta)$ is jointly measurable (it is in fact continuous) if X has continuous sample paths. Then, by Tonelli's theorem (e.g. Folland, 1999, Theorem 2.37), the function

$$\theta \mapsto \int_{\mathcal{Y}} f(y|X, \theta)\mathbf{1}_{A_1}(y) dy = \mathbb{E}_{P_\theta(Y|X)}[\mathbf{1}_{A_1}(Y)] = P_\theta(Y|X)(A_1)$$

is measurable. Now, if A is a measurable subset of $\mathcal{X} \times \mathcal{Y}$, we have the decomposition

$$P_\theta(X, Y)(A) = \int_{\mathcal{X}} P_\theta(Y|X = x)(A_x) dP(X)(x),$$

where $A_x = \{y \in \mathcal{Y} : (x, y) \in A\}$ is the x -section of A . We just saw that $\theta \mapsto P_\theta(Y|X = x)(A_x)$ is measurable, and thus $\theta \mapsto P_\theta(X, Y)(A)$ is measurable, since integration respects measurability. \square

We also examine more closely the claim that our posterior consistency result can be refined so that the set where consistency may fail is “small” in some sense. Using the notation introduced in Section 3, and considering the Lebesgue measure on Θ_p , denoted by λ_p , we need to impose an additional condition:

Condition 9 (Absolute continuity of λ_p). Under the model implied by (3.3), for all $p \in \mathbb{N}$:

- (i) $\Pi(\mathcal{P} = p) > 0$.
- (ii) $\sum_{\nu \in S_p} \Pi(\theta[\nu] \in B | \mathcal{P} = p) = 0$ implies $\lambda_p(B) = 0$, for all $B \subseteq \Theta_p$ measurable.

The first condition is a somewhat technical requirement. The second condition is met, for example, if $\theta|p$ has a density with respect to the Lebesgue measure that is invariant to permutations of the component labels and positive on all of Θ_p . With these prerequisites in mind, denoting by λ the extension of the Lebesgue measure to Θ , we get the announced result:

Proposition 10. *Assume Condition 3 and Condition 9. Then the conclusion of Theorem 4 remains valid with $\lambda(\Theta \setminus \Theta_*) = 0$.*

Proof. Define Θ_* as in the proof of Theorem 4. Recall that $\Pi(\Theta_*) = 1$, and observe that

$$0 = \Pi(\Theta \setminus \Theta_*) = \sum_{p=1}^{\infty} \Pi(\Theta_p \setminus \Theta_* | \mathcal{P} = p) \Pi(\mathcal{P} = p).$$

Since $\Pi(\mathcal{P} = p) > 0$ for all $p \in \mathbb{N}$ by Condition 9-(i), we have $\Pi(\Theta_p \setminus \Theta_* | \mathcal{P} = p) = 0$ for all p . Now, for $\nu \in S_p$, let μ_p^ν be the distribution of $\theta[\nu] | \mathcal{P} = p$ under the model. Note that $(\Theta_p \setminus \Theta_*)[\nu] = \Theta_p \setminus \Theta_*$ by definition of Θ_* , and thus for all $\nu \in S_p$ it holds that

$$\mu_p^\nu(\Theta_p \setminus \Theta_*) = \mu_p^{\text{id}}(\Theta_p \setminus \Theta_*) = \Pi(\Theta_p \setminus \Theta_* | \mathcal{P} = p) = 0. \quad (\text{B.1})$$

Lastly, Condition 9-(ii) means that $\lambda_p \ll \sum_{\nu \in S_p} \mu_p^\nu$, where \ll denotes absolute continuity, and this together with (B.1) implies that $\lambda_p(\Theta_p \setminus \Theta_*) = 0$. But this is valid for all $p \in \mathbb{N}$, so we can conclude, as claimed, that $\lambda(\Theta \setminus \Theta_*) = \sum_{p=1}^{\infty} \lambda_p(\Theta_p \setminus \Theta_*) = 0$. \square

C Experimentation

C.1 Overview of data sets and comparison algorithms

To generate the simulated data sets for the comparison experiments in Section 4, we used four types of Gaussian process regressors commonly employed in the literature, each with a different covariance function:

BM. A Brownian motion, with kernel $K_1(t, s) = \min\{t, s\}$.

fBM. A fractional Brownian motion, with kernel $K_2(t, s) = 1/2(s^{2H} + t^{2H} - |t - s|^{2H})$ and Hurst parameter $H = 0.8$.

O-U. An Ornstein-Uhlenbeck process, with kernel $K_3(t, s) = e^{-|t-s|}$.

Gaussian. A Gaussian process with a squared exponential kernel (also known as Gaussian kernel), namely $K_4(t, s) = e^{-(t-s)^2/2\nu^2}$, where $\nu = 0.2$.

For the comparison algorithms themselves, we considered several frequentist methods which were selected among popular ones in FDA and machine learning in general. As specified in the main article, variable selection and dimensionality reduction methods are part of a pipeline followed by a standard multiple regression technique. In the linear regression case, we chose the following algorithms:

PLS1. Partial least squares regression (e.g. Abdi, 2010).

Lasso. Linear least squares with l^1 regularization.

FPLS and FPLS1. Functional PLS regression through basis expansion, as in Aguilera et al. (2010).

FLin. Standard L^2 functional linear regression model with fixed basis expansion and regularization.

APLS. Functional partial least squares regression proposed by Delaigle and Hall (2012b).

PLS. Partial least squares for dimension reduction.

PCA. Principal component analysis for dimension reduction.

Manual. Dummy variable selection method with a pre-specified number of components (equispaced on $[0, 1]$).

FPCA. Functional principal component analysis.

Ridge. Linear least squares with l^2 regularization. This is used as the multiple regression that follows variable selection or dimensionality reduction methods.

In the logistic regression case, all the variable selection and dimension reduction techniques from above were also considered, with the addition of the following classification methods:

QDA. Quadratic discriminant analysis.

MDC. Maximum depth classifier (e.g. Ghosh and Chaudhuri, 2005).

Log. Standard multiple logistic regression with l^2 regularization. This is used as a one-stage method and also as the multiple regression that follows variable selection or dimensionality reduction methods.

LDA. Linear discriminant analysis.

FNC. Functional nearest centroid classifier with the L^2 -distance.

FLog. Functional RKHS-based logistic regression algorithm proposed in Berrendero et al. (2023).

FLDA. Implementation of the functional version of linear discriminant analysis proposed in Preda et al. (2007).

FKNN. Functional K-nearest neighbors classifier with the L^2 -distance.

RKVS. RKHS-based variable selection and classification method proposed in Berrendero et al. (2018).

APLS+NC. Functional PLS used as a dimension reduction method, as proposed in Delaigle and Hall (2012a) in combination with the nearest centroid (NC) algorithm.

The main hyperparameters of all these algorithms were selected by 10-fold cross-validation, and for those that have a number of components to select, we set 10 as the maximum value so that comparison with our own methods are fair. In particular, regularization parameters are searched among 20 values in the logarithmic

space $[10^{-4}, 10^4]$, the number of basis elements for cubic spline bases is in $\{4, 5, \dots, 10\}$, the number of basis elements for Fourier bases is one of $\{1, 3, 5, 7, 9\}$, and the number of neighbors in the KNN classifier is in $\{3, 5, 7, 9, 11, 13\}$. Most algorithms have been taken from the libraries *scikit-learn* (Pedregosa et al., 2011) and *scikit-fda* (Ramos-Carreño et al., 2024), the first oriented to machine learning in general and the second to FDA in particular. However, some methods were not found in these packages and had to be implemented from scratch. This is the case of the FLDA, FPLS and APLS methods, which we coded following the corresponding articles.

C.2 Simulations with non-Gaussian regressors

We performed an additional set of experiments in linear and logistic regression in which the regressors are not Gaussian processes (GPs), to see if our methods would hold up in this case. These experiments were run in the same conditions as those reported in the main article.

Functional linear regression

We use a geometric Brownian motion (GBM) as the regressor variable, defined as $X(t) = \exp\{\text{BM}(t)\}$, where $\text{BM}(t)$ is a standard Brownian motion. In this case we consider two data sets, one with a RKHS response and one with an L^2 response, both with the same parameters as in the corresponding data sets in Section 4. The comparison results can be seen in Figure 7: in this case our methods still get better results under the RKHS model, while the results under the L^2 -model are essentially the same, which is a positive outcome.

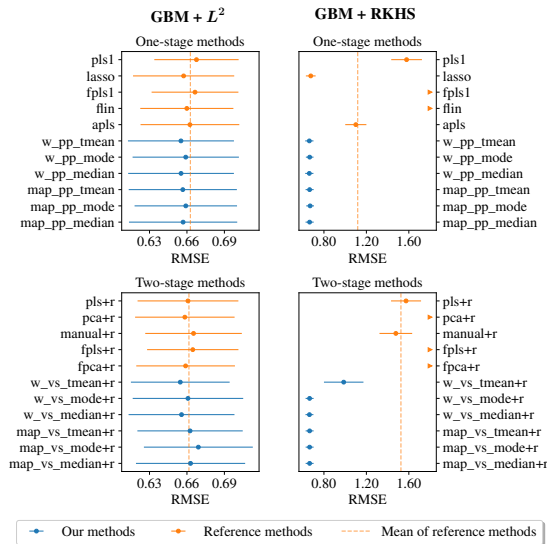


Figure 7: Mean and standard error of RMSE of predictors (lower is better) for 10 runs with GBM regressors. In the first column the response obeys a linear L^2 -model, while in the second column it follows a linear RKHS model.

Functional logistic regression

We consider a “mixture” situation in which we combine regressors from two different GPs with equal probability and label them according to their origin. First, we consider a homoscedastic case to distinguish between a standard Brownian motion and a Brownian motion with a mean function that is zero until $t = 0.5$, and then becomes $m(t) = 0.75t$. Secondly, we consider a heteroscedastic case to distinguish between a standard Brownian motion and a Brownian motion with variance 2, that is, with kernel $K(t, s) = 2 \min\{t, s\}$.

Figure 8 shows that our classifiers perform better than most comparison algorithms in both cases. The differences are most notable in the homoscedastic case, and in the heteroscedastic case the overall accuracy is low. Incidentally, this heteroscedastic case of two zero-mean Brownian motions has a special interest, since it can be shown that the Bayes error is zero in the limit of dense monitoring (i.e. with an arbitrarily fine measurement grid), a manifestation of the “near-perfect” classification phenomenon analyzed for example in Torrecilla et al. (2020). Our results are in line with the empirical studies of this article, where the authors

conclude that even though the asymptotic theoretical error is zero, most classification methods are suboptimal in practice (possibly due to the high collinearity of the data), with the notable exception of PCA+QDA.

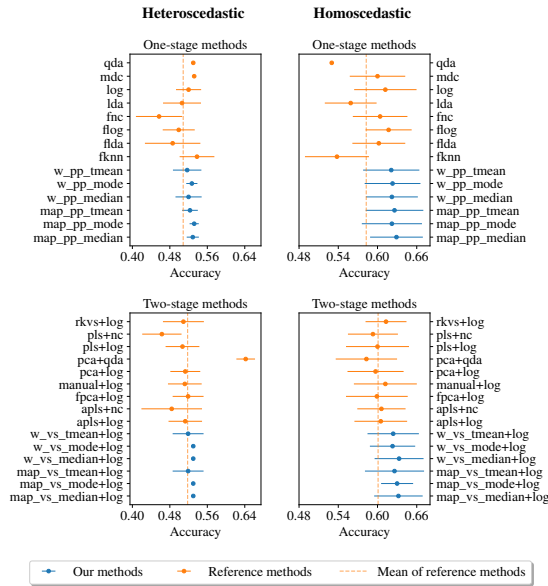


Figure 8: Mean and standard error of accuracy of classifiers (higher is better) for 10 runs with a mix of regressors coming from two different GPs and labeled according to their origin. In the first column we try to separate two Brownian motions with the same mean but different variance, while in the second column we discriminate between two Brownian motions with different mean functions but the same variance.

C.3 Analysis and validation of a model

We give an example through a series of visual representations of how one would analyze the outcome of our Bayesian methods. This is a preliminary step that comes before prediction; the idea is to validate the model and make sure that the resulting samples from the posterior are coherent and useful. For this illustration we consider a data set used in the experiments, for example the one with squared exponential GP regressors, and an underlying linear RKHS response given by (Figure 9)

$$Y = 5 - 5X(0.1) + 5X(0.6) + 10X(0.8) + \varepsilon,$$

with $\varepsilon \sim \mathcal{N}(0, 0.5)$. We run the sampler for 3000 iterations and discard the first 2000, with a Poisson(3) prior truncated to $\{1, \dots, 5\}$ for p .

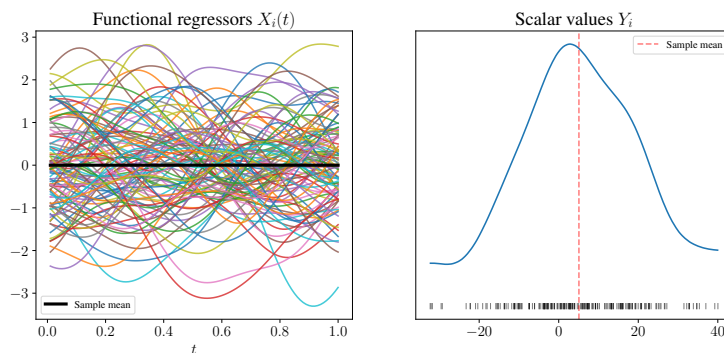


Figure 9: Data set with squared exponential GP regressors and linear RKHS response.

The first thing we do is look at arbitrary samples in the last iteration of a few chains, to check that we get reasonable values. Then, we examine the acceptance rate of all the moves to see that they are not either very

low or very high. Lastly, we compute the so-called Gelman-Rubin statistic (Gelman and Rubin, 1992), which is a quantitative measurement of the convergence of the chains (it should be near 1).

Next we proceed with the visual checks. We can look at the flat posterior distribution of all parameters for all values of p and all the chains aggregated together (Figure 10), or visualize the traces of individual parameters for all values of p (Figure 11). In addition, we can also look at the posterior of the multidimensional parameters for each p in a sort of triangular configuration (Figure 12).

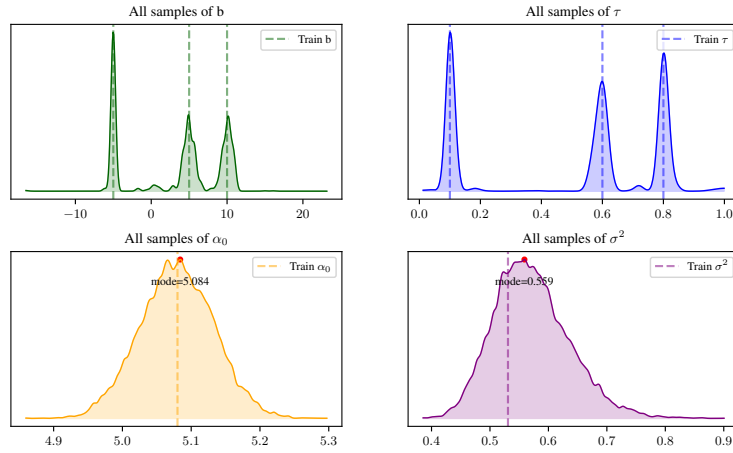


Figure 10: Aggregated posterior distribution of all the samples $\theta_{p_m}^*$ for all m . Note that the true values of the parameters are essentially recovered.

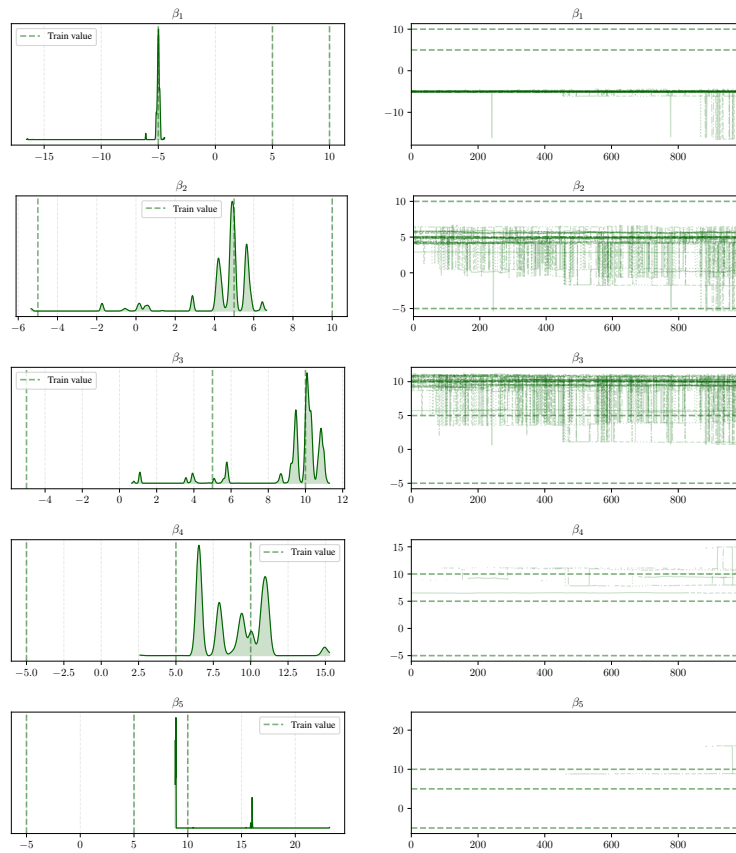


Figure 11: Posterior distribution (left) and trace (right) of all the β_j^* , combined for all p .

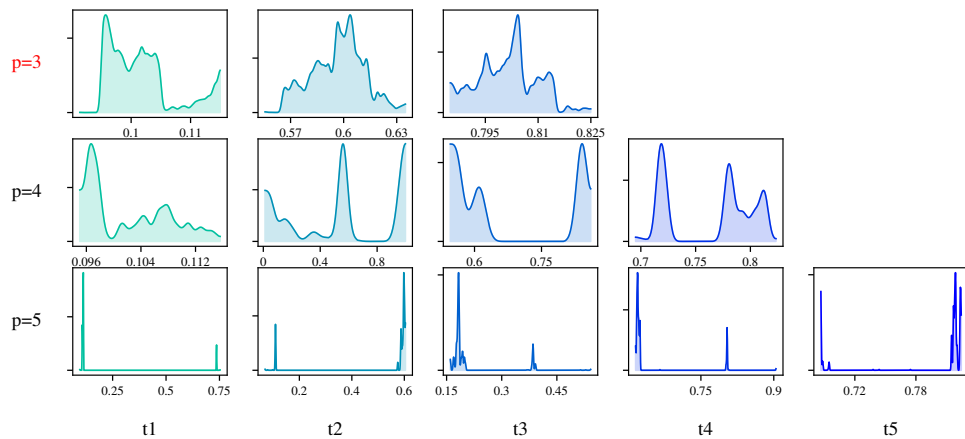


Figure 12: Posterior distribution of τ_p^* for each p . The most frequent value is $p = 3$, highlighted in red. In this run there were no samples with $p = 1$ or $p = 2$ after burn-in.

Looking at the traces is useful to check that the chains are mixing well and that they are correctly exploring the parameter space. We can do the same thing with the posterior values of p (Figure 13). Moreover, we can visualize the tempered posterior distribution of p , that is, the posterior distribution of p for each temperature (Figure 14).

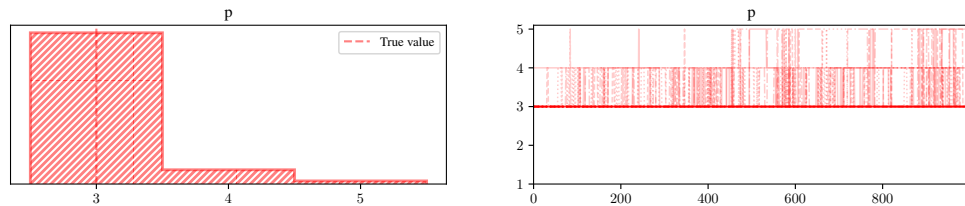


Figure 13: Posterior distribution (left) and trace (right) of p . We see that the true number of components is recovered.

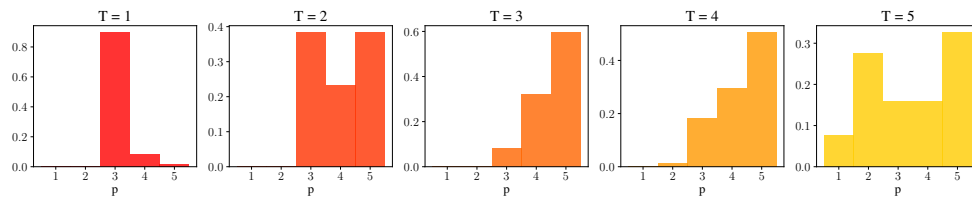


Figure 14: Tempered posterior distribution of p . We are only interested in the cold chain ($T = 1$), but by allowing different temperatures we increase the exploration of the parameter space, periodically transferring some of this information to the cold chain.

Lastly, we can perform a posterior predictive check (Figure 15). This is arguably the most useful visual test for prediction purposes, since we represent the posterior predictive distribution that will be used for inference and prediction. We can do it on the training data or directly on previously unseen regressors. If the sampling has been successful, the posterior predictive distribution should look like a tubular region around the observed data.

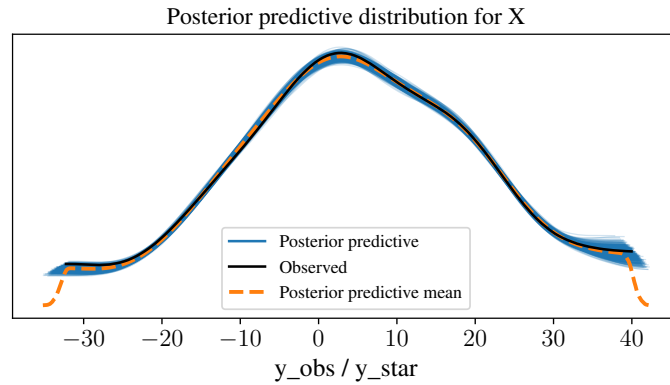


Figure 15: Posterior predictive distribution $Y|X, \theta_{p_m}^*$ for each individual chain m , along with the mean of all chains and the actual observed data Y .

C.4 Tables of experimental results

Here we present the tables corresponding to the empirical comparison studies in Appendix C.2 and in Section 4, which show the numerical values that were depicted there graphically. In each case the best and second-best results are shown in **bold** and **blue**, respectively.

Functional linear regression

Prediction method	BM	fBM	O-U	Gaussian
pls1	0.997 (0.051)	0.730 (0.042)	1.065 (0.055)	0.673 (0.045)
lasso	0.680 (0.044)	0.688 (0.031)	0.684 (0.031)	0.671 (0.042)
fppls1	1.607 (0.078)	0.751 (0.040)	2.088 (0.099)	0.670 (0.046)
f1in	1.829 (0.073)	0.869 (0.037)	2.388 (0.078)	0.957 (0.044)
apls	0.875 (0.053)	0.704 (0.044)	1.005 (0.050)	0.672 (0.045)
w_pp_tmean	0.668 (0.043)	0.676 (0.032)	0.676 (0.042)	0.662 (0.040)
w_pp_mode	0.670 (0.041)	0.676 (0.030)	0.675 (0.041)	0.664 (0.040)
w_pp_median	0.668 (0.043)	0.676 (0.032)	0.676 (0.042)	0.662 (0.040)
map_pp_tmean	0.669 (0.042)	0.677 (0.031)	0.671 (0.045)	0.666 (0.039)
map_pp_mode	0.672 (0.041)	0.680 (0.029)	0.672 (0.045)	0.670 (0.042)
map_pp_median	0.670 (0.043)	0.677 (0.031)	0.670 (0.045)	0.667 (0.040)
pls+r	0.996 (0.056)	0.720 (0.036)	1.065 (0.055)	0.674 (0.044)
pca+r	1.521 (0.070)	0.720 (0.034)	2.249 (0.095)	0.673 (0.045)
manual+r	1.342 (0.130)	0.717 (0.040)	1.719 (0.101)	0.674 (0.042)
fppls+r	1.607 (0.078)	0.752 (0.039)	2.089 (0.098)	0.669 (0.046)
fpca+r	1.512 (0.071)	0.721 (0.034)	2.237 (0.096)	0.673 (0.045)
w_vs_tmean+r	0.795 (0.069)	0.697 (0.029)	0.987 (0.131)	0.672 (0.037)
w_vs_mode+r	0.668 (0.040)	0.678 (0.034)	0.667 (0.041)	0.680 (0.050)
w_vs_median+r	0.668 (0.039)	0.681 (0.031)	0.666 (0.041)	0.666 (0.041)
map_vs_tmean+r	0.668 (0.040)	0.747 (0.048)	0.971 (0.398)	0.737 (0.093)
map_vs_mode+r	0.668 (0.040)	0.679 (0.034)	0.668 (0.042)	0.707 (0.037)
map_vs_median+r	0.668 (0.040)	0.695 (0.029)	0.664 (0.041)	0.700 (0.063)

Table 1: Mean RMSE of predictors (lower is better) for 10 runs with GP regressors, one on each column, that obey an underlying linear RKHS model. The corresponding standard errors are shown between brackets.

Prediction method	BM	fBM	O-U	Gaussian
pls1	0.678 (0.039)	0.674 (0.030)	0.682 (0.043)	0.669 (0.047)
lasso	0.667 (0.037)	0.664 (0.035)	0.659 (0.039)	0.664 (0.041)
fpls1	0.671 (0.041)	0.671 (0.044)	0.677 (0.037)	0.671 (0.048)
flin	0.666 (0.037)	0.664 (0.038)	0.662 (0.038)	0.661 (0.040)
apls	0.673 (0.045)	0.684 (0.043)	0.681 (0.043)	0.674 (0.041)
w_pp_tmean	0.652 (0.037)	0.659 (0.039)	0.651 (0.037)	0.661 (0.039)
w_pp_mode	0.655 (0.037)	0.661 (0.038)	0.652 (0.037)	0.661 (0.039)
w_pp_median	0.652 (0.037)	0.659 (0.039)	0.651 (0.037)	0.661 (0.039)
map_pp_tmean	0.654 (0.037)	0.661 (0.038)	0.655 (0.038)	0.661 (0.039)
map_pp_mode	0.655 (0.035)	0.664 (0.039)	0.656 (0.037)	0.662 (0.037)
map_pp_median	0.654 (0.037)	0.661 (0.038)	0.655 (0.038)	0.661 (0.039)
pls+r	0.667 (0.037)	0.669 (0.033)	0.669 (0.037)	0.665 (0.044)
pca+r	0.665 (0.041)	0.664 (0.041)	0.665 (0.041)	0.666 (0.044)
manual+r	0.665 (0.035)	0.660 (0.037)	0.664 (0.040)	0.666 (0.046)
fpls+r	0.666 (0.040)	0.664 (0.042)	0.672 (0.036)	0.668 (0.047)
fpca+r	0.665 (0.042)	0.665 (0.042)	0.663 (0.040)	0.666 (0.045)
w_vs_tmean+r	0.651 (0.038)	0.660 (0.039)	0.649 (0.036)	0.675 (0.039)
w_vs_mode+r	0.660 (0.037)	0.662 (0.039)	0.663 (0.032)	0.673 (0.046)
w_vs_median+r	0.652 (0.036)	0.660 (0.038)	0.653 (0.039)	0.672 (0.039)
map_vs_tmean+r	0.654 (0.037)	0.661 (0.037)	0.659 (0.039)	0.674 (0.041)
map_vs_mode+r	0.661 (0.036)	0.667 (0.040)	0.670 (0.036)	0.704 (0.058)
map_vs_median+r	0.655 (0.035)	0.663 (0.035)	0.662 (0.043)	0.678 (0.042)

Table 2: Mean RMSE of predictors (lower is better) for 10 runs with GP regressors, one on each column, that obey an underlying linear L^2 -model. The corresponding standard errors are shown between brackets.

Prediction method	GBM + L^2	GBM + RKHS
pls1	0.668 (0.034)	1.579 (0.145)
lasso	0.657 (0.041)	0.676 (0.046)
fppls1	0.666 (0.035)	2.654 (0.182)
flin	0.660 (0.037)	3.434 (0.384)
apls	0.662 (0.040)	1.100 (0.100)
w_pp_tmean	0.655 (0.042)	0.662 (0.039)
w_pp_mode	0.659 (0.043)	0.666 (0.036)
w_pp_median	0.655 (0.042)	0.662 (0.039)
map_pp_tmean	0.657 (0.043)	0.665 (0.038)
map_pp_mode	0.659 (0.041)	0.670 (0.037)
map_pp_median	0.657 (0.043)	0.665 (0.038)
pls+r	0.661 (0.040)	1.574 (0.141)
pca+r	0.658 (0.040)	2.315 (0.195)
manual+r	0.665 (0.039)	1.478 (0.154)
fppls+r	0.665 (0.037)	2.669 (0.189)
fpca+r	0.659 (0.040)	2.311 (0.194)
w_vs_tmean+r	0.655 (0.040)	0.986 (0.186)
w_vs_mode+r	0.661 (0.044)	0.665 (0.038)
w_vs_median+r	0.656 (0.042)	0.663 (0.037)
map_vs_tmean+r	0.662 (0.042)	0.665 (0.038)
map_vs_mode+r	0.669 (0.044)	0.665 (0.038)
map_vs_median+r	0.663 (0.044)	0.665 (0.038)

Table 3: Mean RMSE of predictors (lower is better) for 10 runs with GBM regressors. In the first column the response obeys a linear L^2 -model, while in the second column it follows a linear RKHS model. The corresponding standard errors are shown between brackets.

Prediction method	Moisture	Sugar	Tecator
pls1	0.232 (0.024)	2.037 (0.219)	2.606 (0.283)
lasso	0.242 (0.026)	1.985 (0.226)	2.842 (0.352)
fpls1	0.248 (0.022)	1.972 (0.201)	2.605 (0.262)
flin	1.235 (0.138)	1.966 (0.198)	7.486 (0.648)
apls	0.237 (0.028)	2.020 (0.226)	2.641 (0.165)
w_pp_tmean	0.223 (0.018)	1.988 (0.216)	2.721 (0.260)
w_pp_mode	0.222 (0.020)	1.996 (0.219)	2.718 (0.266)
w_pp_median	0.223 (0.018)	1.989 (0.217)	2.721 (0.262)
map_pp_tmean	0.228 (0.021)	1.997 (0.212)	2.724 (0.267)
map_pp_mode	0.236 (0.023)	2.010 (0.210)	2.741 (0.271)
map_pp_median	0.228 (0.021)	1.996 (0.212)	2.720 (0.267)
pls+r	0.225 (0.021)	1.998 (0.208)	2.536 (0.236)
pca+r	0.233 (0.024)	2.034 (0.219)	2.712 (0.183)
manual+r	0.268 (0.021)	2.041 (0.214)	2.586 (0.270)
fpls+r	0.241 (0.018)	1.962 (0.202)	2.595 (0.249)
fpca+r	0.307 (0.055)	2.054 (0.226)	2.657 (0.189)
w_vs_tmean+r	0.308 (0.075)	2.003 (0.221)	2.822 (0.323)
w_vs_mode+r	0.236 (0.018)	2.050 (0.221)	2.713 (0.255)
w_vs_median+r	0.236 (0.025)	2.000 (0.217)	2.801 (0.261)
map_vs_tmean+r	0.455 (0.284)	2.059 (0.233)	2.900 (0.403)
map_vs_mode+r	0.261 (0.029)	2.188 (0.321)	2.833 (0.291)
map_vs_median+r	0.266 (0.030)	2.082 (0.219)	2.826 (0.269)

Table 4: Mean RMSE of predictors (lower is better) for 10 runs with real data sets, one on each column. The corresponding standard errors are shown between brackets.

Functional logistic regression

Classification method	BM	fBM	O-U	Gaussian
qda	0.510 (0.000)	0.510 (0.000)	0.510 (0.000)	0.500 (0.000)
mdc	0.804 (0.034)	0.822 (0.022)	0.735 (0.037)	0.839 (0.045)
log	0.849 (0.031)	0.848 (0.015)	0.824 (0.022)	0.868 (0.036)
lda	0.694 (0.032)	0.621 (0.066)	0.624 (0.042)	0.823 (0.028)
fnc	0.814 (0.034)	0.848 (0.014)	0.736 (0.035)	0.864 (0.046)
flog	0.845 (0.036)	0.837 (0.024)	0.809 (0.028)	0.871 (0.033)
flda	0.846 (0.031)	0.830 (0.029)	0.813 (0.029)	0.854 (0.039)
fknn	0.851 (0.033)	0.834 (0.027)	0.799 (0.024)	0.847 (0.041)
w_pp_tmean	0.856 (0.030)	0.846 (0.011)	0.828 (0.022)	0.873 (0.035)
w_pp_mode	0.853 (0.031)	0.847 (0.012)	0.825 (0.025)	0.878 (0.036)
w_pp_median	0.856 (0.029)	0.847 (0.011)	0.827 (0.022)	0.873 (0.035)
map_pp_tmean	0.854 (0.034)	0.845 (0.013)	0.830 (0.025)	0.874 (0.035)
map_pp_mode	0.852 (0.032)	0.846 (0.014)	0.829 (0.025)	0.877 (0.036)
map_pp_median	0.855 (0.030)	0.844 (0.013)	0.830 (0.025)	0.876 (0.036)
rkvs+log	0.848 (0.024)	0.838 (0.026)	0.790 (0.032)	0.872 (0.041)
pls+nc	0.816 (0.038)	0.828 (0.022)	0.793 (0.029)	0.867 (0.039)
pls+log	0.847 (0.034)	0.844 (0.021)	0.817 (0.022)	0.864 (0.037)
pca+qda	0.839 (0.034)	0.840 (0.018)	0.818 (0.026)	0.854 (0.033)
pca+log	0.842 (0.032)	0.847 (0.016)	0.824 (0.019)	0.868 (0.033)
manual+log	0.846 (0.032)	0.850 (0.012)	0.821 (0.018)	0.869 (0.032)
fpca+log	0.847 (0.030)	0.847 (0.014)	0.830 (0.024)	0.866 (0.036)
apls+nc	0.819 (0.036)	0.847 (0.014)	0.816 (0.027)	0.854 (0.036)
apls+log	0.829 (0.041)	0.844 (0.012)	0.816 (0.027)	0.857 (0.039)
w_vs_tmean+log	0.831 (0.038)	0.840 (0.017)	0.823 (0.033)	0.873 (0.038)
w_vs_mode+log	0.846 (0.021)	0.828 (0.019)	0.806 (0.020)	0.875 (0.040)
w_vs_median+log	0.838 (0.029)	0.844 (0.017)	0.834 (0.030)	0.875 (0.039)
map_vs_tmean+log	0.816 (0.028)	0.838 (0.023)	0.801 (0.027)	0.876 (0.040)
map_vs_mode+log	0.839 (0.022)	0.831 (0.022)	0.807 (0.014)	0.877 (0.043)
map_vs_median+log	0.829 (0.024)	0.839 (0.019)	0.816 (0.034)	0.871 (0.048)

Table 5: Mean accuracy of classifiers (higher is better) for 10 runs with GP regressors, one on each column, that obey an underlying logistic RKHS model. The corresponding standard errors are shown between brackets.

Classification method	BM	fBM	O-U	Gaussian
qda	0.610 (0.000)	0.610 (0.000)	0.620 (0.000)	0.610 (0.000)
mdc	0.602 (0.033)	0.619 (0.048)	0.615 (0.029)	0.603 (0.042)
log	0.594 (0.017)	0.577 (0.039)	0.591 (0.024)	0.609 (0.037)
lda	0.507 (0.030)	0.518 (0.029)	0.541 (0.039)	0.591 (0.033)
fnc	0.607 (0.038)	0.614 (0.045)	0.609 (0.029)	0.625 (0.040)
flog	0.580 (0.020)	0.602 (0.037)	0.600 (0.031)	0.609 (0.028)
flda	0.601 (0.027)	0.609 (0.049)	0.593 (0.032)	0.595 (0.048)
fknn	0.587 (0.056)	0.576 (0.033)	0.564 (0.042)	0.578 (0.041)
w_pp_tmean	0.597 (0.027)	0.600 (0.026)	0.592 (0.023)	0.608 (0.035)
w_pp_mode	0.599 (0.028)	0.606 (0.027)	0.595 (0.030)	0.605 (0.034)
w_pp_median	0.597 (0.023)	0.599 (0.030)	0.591 (0.020)	0.607 (0.037)
map_pp_tmean	0.595 (0.022)	0.599 (0.027)	0.594 (0.020)	0.602 (0.037)
map_pp_mode	0.605 (0.027)	0.604 (0.030)	0.602 (0.030)	0.606 (0.041)
map_pp_median	0.593 (0.026)	0.599 (0.028)	0.600 (0.023)	0.602 (0.034)
rkvs+log	0.569 (0.039)	0.586 (0.026)	0.593 (0.035)	0.611 (0.034)
pls+nc	0.610 (0.033)	0.623 (0.042)	0.607 (0.035)	0.629 (0.036)
pls+log	0.590 (0.029)	0.589 (0.036)	0.593 (0.020)	0.621 (0.043)
pca+qda	0.577 (0.036)	0.615 (0.032)	0.599 (0.043)	0.618 (0.045)
pca+log	0.590 (0.027)	0.593 (0.027)	0.598 (0.037)	0.616 (0.036)
manual+log	0.580 (0.026)	0.585 (0.030)	0.593 (0.019)	0.621 (0.044)
fpca+log	0.599 (0.021)	0.592 (0.034)	0.600 (0.039)	0.614 (0.042)
apls+nc	0.593 (0.024)	0.569 (0.047)	0.591 (0.039)	0.615 (0.023)
apls+log	0.571 (0.030)	0.585 (0.033)	0.594 (0.025)	0.614 (0.038)
w_vs_tmean+log	0.588 (0.034)	0.594 (0.022)	0.596 (0.017)	0.605 (0.029)
w_vs_mode+log	0.597 (0.024)	0.597 (0.028)	0.601 (0.026)	0.617 (0.026)
w_vs_median+log	0.591 (0.030)	0.589 (0.023)	0.599 (0.035)	0.600 (0.031)
map_vs_tmean+log	0.590 (0.031)	0.594 (0.026)	0.589 (0.030)	0.609 (0.031)
map_vs_mode+log	0.597 (0.024)	0.593 (0.022)	0.599 (0.027)	0.617 (0.021)
map_vs_median+log	0.587 (0.036)	0.592 (0.021)	0.598 (0.036)	0.605 (0.034)

Table 6: Mean accuracy of classifiers (higher is better) for 10 runs with GP regressors, one on each column, that obey an underlying logistic L^2 -model. The corresponding standard errors are shown between brackets.

Classification method	Heteroscedastic	Homoscedastic
qda	0.530 (0.000)	0.530 (0.000)
mdc	0.532 (0.004)	0.600 (0.042)
log	0.520 (0.027)	0.612 (0.048)
lda	0.506 (0.041)	0.559 (0.040)
fnc	0.457 (0.049)	0.604 (0.042)
flog	0.499 (0.034)	0.617 (0.035)
flda	0.486 (0.059)	0.602 (0.040)
fknn	0.538 (0.037)	0.538 (0.049)
w_pp_tmean	0.517 (0.030)	0.621 (0.043)
w_pp_mode	0.527 (0.012)	0.623 (0.043)
w_pp_median	0.520 (0.028)	0.622 (0.040)
map_pp_tmean	0.523 (0.017)	0.626 (0.044)
map_pp_mode	0.532 (0.010)	0.622 (0.046)
map_pp_median	0.529 (0.013)	0.629 (0.040)
rkvs+log	0.509 (0.044)	0.613 (0.031)
pls+nc	0.463 (0.042)	0.593 (0.038)
pls+log	0.507 (0.036)	0.600 (0.048)
pca+qda	0.642 (0.020)	0.583 (0.047)
pca+log	0.513 (0.032)	0.597 (0.043)
manual+log	0.512 (0.036)	0.612 (0.048)
fpca+log	0.519 (0.033)	0.599 (0.047)
apls+nc	0.484 (0.065)	0.606 (0.037)
apls+log	0.513 (0.036)	0.605 (0.040)
w_vs_tmean+log	0.519 (0.033)	0.624 (0.039)
w_vs_mode+log	0.530 (0.000)	0.623 (0.035)
w_vs_median+log	0.530 (0.000)	0.633 (0.037)
map_vs_tmean+log	0.519 (0.033)	0.626 (0.045)
map_vs_mode+log	0.530 (0.000)	0.630 (0.024)
map_vs_median+log	0.530 (0.000)	0.632 (0.037)

Table 7: Mean accuracy of classifiers (higher is better) for 10 runs with a mix of regressors coming from two different GPs and labeled according to their origin. In the first column we try to separate two heteroscedastic Brownian motions, while in the second column we discriminate between two homoscedastic Brownian motions. The corresponding standard errors are shown between brackets.

Classification method	Growth	Medflies	Phoneme
qda	0.581 (0.000)	0.579 (0.028)	0.578 (0.034)
mdc	0.694 (0.103)	0.526 (0.024)	0.704 (0.042)
log	0.961 (0.028)	0.575 (0.022)	0.809 (0.052)
lda	0.894 (0.054)	0.576 (0.016)	0.599 (0.049)
fnc	0.735 (0.117)	0.550 (0.040)	0.755 (0.065)
flog	0.926 (0.043)	0.596 (0.026)	0.785 (0.053)
flda	0.939 (0.051)	0.550 (0.023)	0.782 (0.046)
fknn	0.948 (0.036)	0.539 (0.028)	0.796 (0.035)
w_pp_tmean	0.948 (0.041)	0.611 (0.029)	0.790 (0.037)
w_pp_mode	0.935 (0.046)	0.603 (0.033)	0.790 (0.041)
w_pp_median	0.952 (0.036)	0.610 (0.029)	0.794 (0.041)
map_pp_tmean	0.945 (0.046)	0.606 (0.035)	0.791 (0.031)
map_pp_mode	0.935 (0.046)	0.601 (0.040)	0.779 (0.039)
map_pp_median	0.952 (0.036)	0.606 (0.038)	0.791 (0.031)
rkvs+log	0.929 (0.050)	0.589 (0.032)	0.804 (0.046)
pls+nc	0.858 (0.090)	0.558 (0.032)	0.776 (0.058)
pls+log	0.945 (0.032)	0.574 (0.019)	0.810 (0.043)
pca+qda	0.955 (0.030)	0.576 (0.025)	0.754 (0.043)
pca+log	0.958 (0.035)	0.562 (0.028)	0.793 (0.049)
manual+log	0.932 (0.055)	0.615 (0.012)	0.730 (0.046)
fpca+log	0.955 (0.033)	0.561 (0.024)	0.769 (0.050)
apls+nc	0.961 (0.028)	0.551 (0.030)	0.781 (0.047)
apls+log	0.952 (0.036)	0.562 (0.015)	0.776 (0.048)
w_vs_tmean+log	0.961 (0.028)	0.597 (0.036)	0.749 (0.071)
w_vs_mode+log	0.948 (0.046)	0.597 (0.025)	0.804 (0.037)
w_vs_median+log	0.952 (0.033)	0.597 (0.021)	0.779 (0.049)
map_vs_tmean+log	0.945 (0.046)	0.592 (0.047)	0.746 (0.066)
map_vs_mode+log	0.948 (0.046)	0.592 (0.036)	0.779 (0.035)
map_vs_median+log	0.939 (0.047)	0.592 (0.031)	0.782 (0.050)

Table 8: Mean accuracy of classifiers (higher is better) for 10 runs with real data sets, one on each column. The corresponding standard errors are shown between brackets.

D Source code overview

The Python code developed for this work is available under a GPLv3 license at the GitHub repository <https://github.com/antcc/rk-bfr-jump>. The code is adequately documented and is structured in several directories as follows:

- In the `rkbfr_jump` folder we find the files responsible for the implementation of our Bayesian models, separated according to the functionality they provide. There is also a `utils` folder inside with some utility files for simulation, experimentation and visualization.
- The `reference_methods` folder contains our implementation of the functional comparison algorithms that were not available through a standard Python library.
- The `experiments` folder contains plain text files with the numerical experimental results shown in Appendix C.4, as well as `.csv` files that facilitate working with them.
- At the root folder we have a Python script `experiments.py` for executing our experiments, which accepts several user-specified parameters (such as the number of iterations or the type of data set). There is also a `setup.py` file to install our method as a Python package.

When possible, the code was implemented in a generic way that would allow for easy extensions or derivations. It was also developed with efficiency in mind, so many functions and methods exploit the vectorization capabilities of the `numpy` and `scipy` libraries, and are sometimes parallelized using `numba`. Moreover, since we followed closely the style of the `scikit-learn` and `scikit-fda` libraries, our methods are compatible and could be integrated (after some minor tweaking) with both of them.

The code for the experiments was executed with a random seed set to the value 2024 for reproducibility. We provide a script file `launch.sh` that illustrates a typical execution. Lastly, there are *Jupyter* notebooks that demonstrate the use of our methods in a more visual way. Inside these notebooks there is a step-by-step guide on how one might execute our algorithms, accompanied by many graphical representations, and offering the possibility of changing multiple parameters to experiment with the code. In addition, there is also a notebook that can be used to generate all the tables and figures of this document and the main article pertaining to the experimental results.